J Eng Math (2007) 59:25–60
DOI 10.1007/s10665-006-9058-x

ORIGINAL ARTICLE

Numerical treatment of a skew-derivative problem for the Laplace equation in the exterior of an open arc

P. A. Krutitskii · D. Y. Kwak · Y. K. Hyon

Received: 9 September 2005 / Accepted: 15 May 2006 / Published online: 11 January 2007

Abstract The skew-derivative problem for harmonic functions in the exterior of an open arc in a plane is considered. This problem models the electric current in a semiconductor film from an electrode of arbitrary shape in the presence of a magnetic field. A numerical method for solving the problem is proposed. The method is based on a boundary-integral-equation approach. The proposed numerical method is tested. The numerical simulation is presented for different values of the parameters and different shapes of the electrode. Physical effects found in numerical experiments are discussed.

Keywords Boundary-integral equation · Laplace equation · Numerical methods · Semiconductor · Skew derivative

1 Introduction

Boundary-value problems for the Laplace equation in the exterior of an open arc with Dirichlet and Neumann boundary conditions are of great practical importance, since they have applications in hydrodynamics, electrostatics, thermodynamics, etc. Modern numerical methods for the analysis of these problems are presented in [1, Chapters 4, 17], [2, Chapters 4, 9], where the reader may find further references. The numerical methods discussed in [1, Chapters 4, 17], [2, Chapters 4, 9] are based on boundary-integral-equation approaches and involve a numerical treatment of singular integral equations as well as the computation of single- and double-layer potentials for the Laplace equation. The present paper is devoted to the numerical analysis of the skew-derivative problem for the Laplace equation in the exterior of an

P. A. Krutitskii (✉)
Department of Mathematics, Moscow State University,
Moscow, 119899, Russia
e-mail: krutitsk@math.phys.msu.su

D. Y. Kwak · Y. K. Hyon
Department of Mathematics, Korea Advanced Institute of Science and Technology,
373-1, Guseong-dong, Yuseong-gu, Daejeon 305-701, Republic of Korea

open arc in a plane. This problem has not been treated numerically before. A numerical method for finding a computational solution of this problem is suggested in the present paper.

From a physical standpoint, we treat a problem concerning an electric current in a semiconductor film from an electrode of arbitrary shape with a magnetic field that is orthogonal to the film. The directions of electric current and electric intensity do not coincide in this model in the case of a non-zero magnetic field. This phenomenon is known in physics as the Hall effect [3], [4, Sects. 1, 2, 3], [5, Sect. 4], [6, Part 1]. The physical problem is reduced to a skew-derivative problem for two-dimensional harmonic functions in the exterior of an open arc, which models an electrode, in a plane. The existence and uniqueness of the solution to this problem are proved in [7]. The integral representation of the solution to the problem is obtained in [7] in the form of potentials with the density satisfying a uniquely solvable Fredholm integral equation of the second kind. In the present paper, a numerical method for solving this problem is proposed based on the approach developed in [7]. The numerical method consists of two steps. The first step is to find the density in the potentials by numerically solving the Fredholm integral equation with the help of its discretization and inversion of the matrix. We tested the numerical method for solving the integral equation by comparison with explicit solutions which are obtained in the present paper for certain cases. It is found that the convergence of the numerical solution of the integral equation is $O(h^{3/2})$. The second step in our numerical method concerns the computation of the potentials by using the density from the previous step. Since the integrands in the potentials include a singular part, we have to treat these singularities. We propose some schemes for dealing with these singularities. To obtain numerical formulas for a logarithmic potential, we evaluate integrals with certain singularities in explicit form and propose a "selection of singularity" scheme. Moreover, we develop a numerical algorithm for the computation of the non-classical angular potential, which is studied in [7–9]. This algorithm is based on finding a fixed branch and "direct computation" of the kernel in the angular potential. Next, this algorithm for the angular potential is improved by dividing each interval of integration in subintervals ("subdivision scheme"). We tested the numerical schemes for the computation of the potentials by comparison with exact values of potentials that are evaluated analytically in the present paper for certain cases. The uniform relative error of the numerical schemes for the potentials is less than two percent if the distance from the arc is more than h, where h is the uniform discretization step of the arc in the computations. In calculating the relative error we drop points, where the absolute value of the exact solution is less than h. Moreover, if the distance from the arc is less than h, the uniform relative error in our method is less than two percent as well. This is an advantage of our method in comparison with known numerical methods for Dirichlet and Neumann harmonic problems in the exterior of an arc in a plane. In the present paper, we use the proposed numerical method for a simulation of the electric parameters (electric potential, intensity and current) in a problem on the electric current from an electrode in a semiconductor film in the presence of a magnetic film. The results of a numerical simulation are presented graphically. A number of interesting physical phenomena are found and discussed in the present paper.

In Sects. 2 and 3 we formulate the problem. The discretization scheme and numerical method for solving the integral equation for the density in the potentials are discussed in Sect. 4. Using results of Sect. 4, we obtain the recovery formulas for the potentials and a remedial scheme for recovering the angular potential in Sect. 5. Finally, we present test results for the numerical method, results of a simulation of electric parameters in a semiconductor film and conclusions in the other three sections.

2 Formulation of the boundary-value problem

In Cartesian coordinates $x = (x_1, x_2) \in R^2$ we consider a plane semiconductor film. Suppose that a constant magnetic field acts in the normal direction to the plane (x_1, x_2). The equations for the electric current in the semiconductor film in a linear case are

$$\mathrm{div}\mathbf{J} = 0, \quad \mathbf{J} = \Lambda\mathbf{E}, \quad \mathbf{E} = -\nabla \mathrm{u},$$

where $\mathbf{J} = (J_1, J_2)$ is the current density, $\mathbf{E}$ is the intensity of the electric field, u is the electric-field potential, Λ is the conductivity tensor

$$\Lambda = \frac{\eta}{1+\beta^2}\begin{pmatrix} 1 & \beta \\ -\beta & 1 \end{pmatrix},$$

where η is the conductivity, $\beta = \eta_1 \mathcal{M}$, η_1 is the mobility of the carriers, and $\mathcal{M}$ is the projection of the magnetic induction onto the x_3-axis. Suppose that η is a positive constant and β is a real constant.

We consider an electrode placed in an unbounded semiconductor film. The electrode is modeled by a simple open curve $\Gamma \in C^{2,\lambda}$, where the Hölder exponent $\lambda \in (0,1]$. By a simple open curve we mean a nonclosed smooth arc of finite length without self-intersections [10, Sect. 1].

We assume that the curve Γ is parametrized by the arc length s:

$$\Gamma = \{x : x = x(s) = (x_1(s), x_2(s)),\ s \in [a,b]\}.$$

Therefore, points $x \in \Gamma$ and values of the parameter s are in one-to-one correspondence.

We denote the tangent vector to Γ at the point $x(s)$ by $\tau_x = (\cos\alpha(s), \sin\alpha(s))$, where $\cos\alpha(s) = x_1'(s)$, $\sin\alpha(s) = x_2'(s)$. Let $n_x = (\sin\alpha(s), -\cos\alpha(s))$ be the normal vector to Γ at $x(s)$.

Suppose that the normal current density is specified at the electrode Γ. According to the equations given above, this model leads to the skew-derivative boundary condition in terms of the electric potential $u(x)$:

$$\begin{aligned}(\mathbf{J}, n_x)|_{x(s)\in\Gamma} &= -\frac{\eta}{1+\beta^2}\left(\frac{\partial u}{\partial n_x} + \beta\frac{\partial u}{\partial \tau_x}\right)\Big|_{x(s)\in\Gamma} \\ &= -\frac{\eta}{1+\beta^2} f(s),\end{aligned}$$

where $f(s)$ is a function specified on $[a,b]$.

The equations presented above are transformed to the 2D Laplace equation with respect to $u(x) = u(x_1, x_2)$. Below, the open curve Γ is considered as a cut in a plane. The side of the cut Γ which is situated on the left when the parameter s increases will be called Γ^+, while the opposite side will be called Γ^-. To give a rigorous mathematical formulation of the skew-derivative problem for the Laplace equation, the following definition of the appropriate smoothness class has been introduced in [7].

Definition 2.1 The function $u(x)$ belongs to the smoothness class $\mathbf{K}$ if this function satisfies the following conditions

(1) $u \in C^2(R^2 \setminus \Gamma)$, u is continuously extensible on the cut Γ from the left and right; besides u is continuous at the ends of Γ;
(2) ∇u is continuously extensible on the cut $\Gamma \setminus X$ from the left and right, where X is a point-set, consisting of the endpoint of Γ, i.e., $X = \{x(a) \cup x(b)\}$;
(3) in the neighborhood of any point $x(d) \in X$ for some constants $\mathcal{C} > 0$, $\epsilon > -1$ the inequality

$$|\nabla u| \le \mathcal{C}|x - x(d)|^{\epsilon} \tag{1}$$

holds, where $x \to x(d)$ and $d = a$ or $d = b$.

In the above definition we imply that $u(x)$ and $\nabla u(x)$ are continuously extensible on the cut $\Gamma \setminus X$ from the left and right, but values of $u(x)$ and $\nabla u(x)$ from the left and right on $\Gamma \setminus X$ may be different, i.e., $u(x)$ and $\nabla u(x)$ may have jumps on $\Gamma \setminus X$.

On the basis of the model described above, the skew-derivative problem is formulated for the Laplace equation in $R^2 \setminus \Gamma$ in [7] as follows:

Problem 2.1 To find a function $u(x)$ of the class **K** which satisfies the Laplace equation

$$\Delta u(x) = 0, \quad x \in R^2 \setminus \Gamma, \tag{2}$$

the boundary condition

$$\left(\frac{\partial}{\partial n_x}u(x(s)) + \beta\frac{\partial}{\partial \tau_x}u(x(s))\right)\Big|_\Gamma = f(s) \tag{3}$$

and the following conditions at infinity

$$\begin{aligned} &|u(x)| \le \text{Const}, \quad |\nabla u(x)| = o(|x|^{-1}), \\ &|x| = \sqrt{x_1^2 + x_2^2} \to \infty. \end{aligned} \tag{4}$$

We suppose that β is a real constant. All conditions of problem 2.1 must be satisfied in the classical sense.

3 Integral equations at the boundary and the solution of the problem

We say, that $\mu(s) \in C^{\omega}_{1/2}[a,b]$ with $\omega \in (0,1]$ if

$$\mu(s)|s-a|^{1/2}|s-b|^{1/2} \in C^{0,\omega}[a,b],$$

where $C^{0,\omega}[a,b]$ is a Hölder space with the exponent ω. The norm in $C^{\omega}_{1/2}[a,b]$ is defined by the equality

$$\|\mu(s)\|_{C^{\omega}_{1/2}[a,b]} = \|\mu(s)|s-a|^{1/2}|s-b|^{1/2}\|_{C^{0,\omega}[a,b]}.$$

We consider the angular potential [7–9] for the Laplace equation (2)

$$v[\mu](x) = -\frac{1}{2\pi}\int_a^b \mu(\sigma)V(x,\sigma)\mathrm{d}\sigma. \tag{5}$$

The kernel $V(x,\sigma)$ is defined (up to indeterminacy $2\pi m,\ m = \pm1, \pm2, \ldots$) by the formulae

$$\cos V(x,\sigma) = \frac{x_1 - y_1(\sigma)}{|x - y(\sigma)|}, \quad \sin V(x,\sigma) = \frac{x_2 - y_2(\sigma)}{|x - y(\sigma)|}, \tag{6}$$

where

$$\begin{aligned} &y(\sigma) = (y_1(\sigma), y_2(\sigma)) \in \Gamma, \\ &|x - y(\sigma)| = \sqrt{(x_1 - y_1(\sigma))^2 + (x_2 - y_2(\sigma))^2}. \end{aligned}$$

By the kernel $V(x,\sigma)$ we denote an arbitrary fixed branch of this function, which varies continuously with σ along the curve Γ for given fixed $x \notin \Gamma$.

Under this definition of $V(x,\sigma)$, the potential $v[\mu](x)$ is a multi-valued function. In order that the potential $v[\mu](x)$ be single-valued, it is necessary to impose the following additional condition:

$$\int_a^b \mu(\sigma)\mathrm{d}\sigma = 0. \tag{7}$$

Integrating the angular potential by parts, we obtain its representation through the double-layer potential as follows [7–9]:

$$v[\mu](x) = \frac{1}{2\pi}\int_a^b \rho(\sigma)\frac{\partial}{\partial n_y}\log|x - y(\sigma)|\mathrm{d}\sigma,$$

where

$$\rho(\sigma) = \int_a^\sigma \mu(\xi)\mathrm{d}\xi, \quad \sigma \in [a,b]. \tag{8}$$

If $f(s)$ from (3) is an arbitrary function from the Banach space $C^{0,\lambda}[a,b]$, where the Hölder exponent $\lambda \in (0,1]$, then the solution of problem 2.1 has been obtained in [7] by potential theory in the following form

$$u[\mu](x) = v[\mu](x) - \beta w[\mu](x) + C, \tag{9}$$

where C is an arbitrary constant, the angular potential $v[\mu](x)$ is defined in (5), and the single-layer potential $w[\mu](x)$ is given by the formula

$$w[\mu](x) = -\frac{1}{2\pi}\int_a^b \mu(\sigma)\log|x - y(\sigma)|\mathrm{d}\sigma. \tag{10}$$

According to [7], the density $\mu(s)$ in (9) is a function that belongs to the space $C^{\omega}_{1/2}[a,b]$ with some $\omega \in (0,1]$, satisfies condition (7) and obeys the following singular integral equation [10, Chapter 5]

$$-\frac{1+\beta^2}{2\pi}\int_a^b \mu(\sigma)\frac{\sin\varphi_0(x(s),y(\sigma))}{|x(s)-y(\sigma)|}\mathrm{d}\sigma = f(s), \quad s \in [a,b], \tag{11}$$

where $\varphi_0(x,y)$ is the angle between the vector $\overrightarrow{xy}$ and the direction of the normal n_x. The angle $\varphi_0(x,y)$ is taken to be positive if it is measured anticlockwise from n_x and negative if it is measured clockwise from n_x. Besides, $\varphi_0(x,y)$ is continuous in $x, y \in \Gamma$ if $x \neq y$.

Equation (11) is obtained in [7] by substituting the potential (9) in the boundary condition (3) and by using limiting formulae for the potentials from [8, 9].

It is shown in [7, Theorem 2] that, if $\mu(s)$ is a solution of the Eqs. (7) and (11) from the space $C^{\omega}_{1/2}[a,b]$, $\omega \in (0,1]$, the potential (9) is a solution of problem 2.1. In particular, the potential (9) belongs to the smoothness class **K**.

The existence and uniqueness of a solution of the system (7), (11) in the Banach space $C^{\omega}_{1/2}[a,b]$ have been proved in [7] by means of a reformulation the system (7), (11) as a Fredholm integral equation of the second kind and index zero.

According to [9, 11],

$$Y(s,\sigma) = \frac{1}{\pi}\left(\frac{\sin\varphi_0(x(s),y(\sigma))}{|x(s)-y(\sigma)|} - \frac{1}{\sigma - s}\right) \in C^{0,\lambda}([a,b]\times[a,b]),$$

so we can rewrite (11) in the following form [7]

$$\frac{1}{\pi}\int_a^b \mu(\sigma)\frac{\mathrm{d}\sigma}{\sigma - s} + \int_a^b \mu(\sigma)Y(s,\sigma)\mathrm{d}\sigma = -\frac{2}{1+\beta^2}f(s), \quad s \in [a,b]. \tag{12}$$

Inverting the singular integral operator in (12), we arrive at the following integral equation of the second kind [7]:

$$\begin{aligned}\mu(s) + \frac{1}{\sqrt{s-a}\sqrt{b-s}}\int_a^b \mu(\sigma)A(s,\sigma)\mathrm{d}\sigma + \frac{1}{\sqrt{s-a}\sqrt{b-s}}G \\ = \frac{1}{\sqrt{s-a}\sqrt{b-s}}\Phi(s), \quad s \in [a,b],\end{aligned} \tag{13}$$

where G is a constant and

$$A(s,\sigma) = -\frac{1}{\pi}\int_a^b \frac{Y(\xi,\sigma)}{\xi - s}\sqrt{\xi - a}\sqrt{b-\xi}\,\mathrm{d}\xi,$$

$$\Phi(s) = \frac{1}{\pi}\left(\frac{1}{1+\beta^2}\right)\int_a^b \frac{2\sqrt{\sigma - a}\sqrt{b-\sigma}f(\sigma)}{\sigma - s}\,\mathrm{d}\sigma.$$

It follows from condition (7) that $G = 0$ (see [7]); therefore Eq. (13) takes the form

$$\mu(s) + \frac{1}{\sqrt{s-a}\sqrt{b-s}} \int_a^b \mu(\sigma) A(s,\sigma) \mathrm{d}\sigma = \frac{1}{\sqrt{s-a}\sqrt{b-s}} \Phi(s), \quad s \in [a,b]. \tag{14}$$

To simplify (14), we introduce the new unknown function

$$\mu_*(s) = \mu(s)\sqrt{s-a}\sqrt{b-s} \in C^{0,\omega}[a,b] \tag{15}$$

and rewrite (14) in the form

$$\mu_*(s) + \int_a^b \mu_*(\sigma) \frac{A(s,\sigma)}{\sqrt{\sigma-a}\sqrt{b-\sigma}} \mathrm{d}\sigma = \Phi(s), \quad s \in [a,b]. \tag{16}$$

Thus, the system of Eqs. (7), (11) for $\mu(s)$ has been reduced to Eq. (16) for the function $\mu_*(s)$. It is clear from our considerations that any solution of (16) gives a solution of system (7), (11) and vice versa.

It is shown in [7] that Eq. (16) has a unique solution $\mu_*(s) \in C^{0,\omega}[a,b]$, $\omega = \min\{\lambda, 1/2\}$, for any $f(s) \in C^{0,\lambda}[a,b]$ subject to the boundary condition (3). Moreover, according to [7], the solution of problem 2.1 is given by formula (9), where C is an arbitrary constant, while $\mu(s) = \mu_*(s)/(\sqrt{s-a}\sqrt{b-s})$, where $\mu_*(s)$ is the unique solution of the integral equation (16) in $C^{0,\omega}[a,b]$. It is shown in [7] that problem 2.1 does not have other solutions.

4 Discretization

To justify the numerical method for the solution of problem 2.1 we will assume that $f(s) \in C^1[a,b]$ in (3).

In this section we consider a discretization of Eq. (16) for a linear algebraic system. It follows from [9] that

$$\frac{\sin\varphi_0(x(s),y(\sigma))}{|x(s)-y(\sigma)|} = -\frac{\partial}{\partial s}\log|x(s)-y(\sigma)| = -\frac{x_1(s)-y_1(\sigma)}{|x(s)-y(\sigma)|^2}\cos\alpha(s) - \frac{x_2(s)-y_2(\sigma)}{|x(s)-y(\sigma)|^2}\sin\alpha(s), \tag{17}$$

since $x_1'(s) = \cos\alpha(s)$, $x_2'(s) = \sin\alpha(s)$.

Using the formula

$$I_0(s) = \frac{1}{\pi}\int_a^b \frac{Q(\sigma)}{\sigma - s}\mathrm{d}\sigma = \frac{a+b}{2} - s, \quad Q(s) = \sqrt{s-a}\sqrt{b-s}, \tag{18}$$

(the derivation of (18) is presented in the Appendix), we have

$$\begin{aligned}\Phi(s) &= \frac{1}{\pi}\left(\frac{1}{1+\beta^2}\right)\int_a^b \frac{2Q(\sigma)}{\sigma-s} f(\sigma)\mathrm{d}\sigma \\ &= \frac{2}{1+\beta^2}\left[\frac{1}{\pi}\int_a^b \frac{Q(\sigma)(f(\sigma)-f(s))}{\sigma-s}\mathrm{d}\sigma + \frac{f(s)}{\pi}\int_a^b \frac{Q(\sigma)}{\sigma-s}\mathrm{d}\sigma\right] \\ &= \frac{2}{1+\beta^2}\left[\frac{1}{\pi}\int_a^b \frac{Q(\sigma)(f(\sigma)-f(s))}{\sigma-s}\mathrm{d}\sigma + f(s)\left(\frac{a+b}{2} - s\right)\right].\end{aligned} \tag{19}$$

Note that $\dfrac{f(\sigma)-f(s)}{\sigma-s}$ is continuous if $f(s) \in C^1[a,b]$. Let $F(s,\sigma) = \dfrac{f(\sigma)-f(s)}{\sigma-s}$; then $F(s,s) = f'(s)$. To compute the integral term in (19), we have to evaluate the $F(s_k,\sigma_k)$ implying that $\sigma_k = s_k$. So, we can use

$F(s_k,\sigma_k) = f'(s_k)$, or $F(s_k,\sigma_k) \approx \dfrac{F(s_k,\sigma_k+\frac{h}{4}) + F(s_k,\sigma_k-\frac{h}{4})}{2}$ if $\sigma_k = s_k$. To compute $F(s_k,\sigma_k \pm \frac{h}{4})$ with $\sigma_k = s_k$, the original formula of $F(s,\sigma)$ can be used since there is no singularity.

Now, using (18), we rewrite $A(s,\sigma)$ in (16) as follows

$$\begin{aligned} A(s,\sigma) &= -\frac{1}{\pi}\int_a^b \frac{Y(\xi,\sigma)-Y(s,\sigma)}{\xi-s}Q(\xi)\mathrm{d}\xi - \frac{Y(s,\sigma)}{\pi}\int_a^b \frac{Q(\xi)}{\xi-s}\mathrm{d}\xi \\ &= -\frac{1}{\pi}\int_a^b \frac{Y(\xi,\sigma)-Y(s,\sigma)}{\xi-s}Q(\xi)\mathrm{d}\xi - Y(s,\sigma)\left[\frac{a+b}{2}-s\right]. \end{aligned}$$

If $\Gamma \in C^3$, one can easily show that $Y(s,\sigma) \in C^1(\Gamma^1 \times \Gamma^1)$ in both variables.

Consider a function $G(\xi,s,\sigma) = \dfrac{Y(\xi,\sigma)-Y(s,\sigma)}{\xi-s}$; then $G(\xi,s,\sigma)$ is continuous in s,σ,ξ on Γ and clearly, $G(s,s,\sigma) = Y'_s(s,\sigma) \in C^0(\Gamma^1 \times \Gamma^1)$. However, it is better for $G(\xi_k,s_k,\sigma_p)$ with $\xi_k = s_k$ to be calculated by the formula

$$G(\xi_k,s_k,\sigma_p) = \frac{G(\xi_k-\frac{h}{4},s_k,\sigma_p) + G(\xi_k+\frac{h}{4},s_k,\sigma_p)}{2}.$$

We consider a uniform discretization of the arc and take all function values at the discretized points s_k,σ_k,ξ_k such that

$$s_k = \sigma_k = \xi_k = a + h\left(k-\frac{1}{2}\right), \quad k = 1,2,\ldots,M,$$

where $h = \dfrac{b-a}{M}$.

Now, we can easily find $\Phi(s_k)$ for all k:

$$\Phi(s_k) = \frac{2}{1+\beta^2}\left[\frac{1}{\pi}\sum_{p=1}^{M} F(s_k,\sigma_p)Q(\sigma_p)h + f(s_k)\left(\frac{a+b}{2}-s_k\right)\right].$$

In this formula

$$F(s_k,\sigma_p) = \begin{cases} \dfrac{f(\sigma_p)-f(s_k)}{\sigma_p-s_k}, & \text{if } p \neq k, \\ \dfrac{1}{2}\left[F\left(s_k,\sigma_p-\dfrac{h}{4}\right) + F\left(s_k,\sigma_p+\dfrac{h}{4}\right)\right], & \text{if } p = k, \end{cases}$$

where $F(s_k,\sigma_p \pm \frac{h}{4}) = \dfrac{f(\sigma_p \pm \frac{h}{4}) - f(s_k)}{\sigma_p \pm \frac{h}{4} - s_k}$.

Similarly, we can find the kernel $A(s_k,\sigma_m)$ for all k,m:

$$A(s_k,\sigma_m) = -\frac{1}{\pi}\sum_{p=1}^{M} G(\xi_p,s_k,\sigma_m)Q(\xi_p)h - Y(s_k,\sigma_m)\left(\frac{a+b}{2}-s_k\right).$$

In this formula

$$G(\xi_p,s_k,\sigma_m) = \begin{cases} \dfrac{Y(\xi_p,\sigma_m)-Y(s_k,\sigma_m)}{\xi_p-s_k}, & \text{if } p \neq k, \\ \dfrac{1}{2}\left[G\left(\xi_k-\dfrac{h}{4},s_k,\sigma_m\right) + G\left(\xi_k+\dfrac{h}{4},s_k,\sigma_m\right)\right], & \text{if } p = k, \end{cases} \tag{20}$$

where $G(\xi_k \pm \frac{h}{4},s_k,\sigma_m) = \dfrac{Y(\xi_k \pm \frac{h}{4},\sigma_m) - Y(s_k,\sigma_m)}{\xi_k \pm \frac{h}{4} - s_k}$. We set

$$Y(s,s) \approx \frac{1}{2}\left[Y\left(s,s-\frac{h}{4}\right) + Y\left(s,s+\frac{h}{4}\right)\right].$$

Hence, we get the discretized equation (16) as follows:

$$\mu_*(s_k) + \sum_{m=1}^{M} \mu_*(\sigma_m) A(s_k, \sigma_m) \int_{\sigma_m - \frac{h}{2}}^{\sigma_m + \frac{h}{2}} \frac{\mathrm{d}\sigma}{Q(\sigma)} = \Phi(s_k), \quad k = 1, 2, \ldots, M. \tag{21}$$

If $m \neq 1, m \neq M$, then

$$\int_{\sigma_m - \frac{h}{2}}^{\sigma_m + \frac{h}{2}} \frac{\mathrm{d}\sigma}{Q(\sigma)} \approx \frac{h}{Q(\sigma_m)}, \tag{22}$$

if $m = 1$, then

$$\int_{\sigma_1 - \frac{h}{2}}^{\sigma_1 + \frac{h}{2}} \frac{\mathrm{d}\sigma}{\sqrt{\sigma - a}\sqrt{b - \sigma}} \approx \frac{2}{\sqrt{b - \sigma_1}} \sqrt{\sigma - a} \Big|_a^{a+h} = \frac{2\sqrt{h}}{\sqrt{b - \sigma_1}}, \tag{23}$$

and if $m = M$, we have

$$\int_{b-h}^{b} \frac{\mathrm{d}\sigma}{\sqrt{\sigma - a}\sqrt{b - \sigma}} \approx \frac{-2}{\sqrt{\sigma_M - a}} \sqrt{b - \sigma} \Big|_{b-h}^{b} = \frac{2\sqrt{h}}{\sqrt{\sigma_M - a}}. \tag{24}$$

Therefore, the discretized equation (16) takes the form

$$\mu_*(s_k) + \sum_{m=1}^{M} \mu_*(\sigma_m) A(s_k, \sigma_m) g(\sigma_m) = \Phi(s_k), \quad k = 1, 2, \ldots, M \tag{25}$$

where

$$g(\sigma_m) = \begin{cases} \dfrac{h}{Q(\sigma_m)}, & \text{if } m \neq 1, m \neq M, \\ \dfrac{2\sqrt{h}}{\sqrt{b - \sigma_1}}, & \text{if } m = 1, \\ \dfrac{2\sqrt{h}}{\sqrt{\sigma_M - a}}, & \text{if } m = M. \end{cases}$$

Finally, we get a linear algebraic system of equations with respect to $\mu_*(s_k)$:

$$W \begin{pmatrix} \mu_*(\sigma_1) \\ \vdots \\ \mu_*(\sigma_M) \end{pmatrix} = \begin{pmatrix} \Phi(s_1) \\ \vdots \\ \Phi(s_M) \end{pmatrix}, \tag{26}$$

where W is the matrix induced from (25). Therefore, we can apply several numerical methods for solving this linear system.

5 Recovery of the potentials $w[\mu](x)$ and $v[\mu](x)$

In this section, we introduce a scheme for calculating the single-layer potential, called "selection of singularity", and a scheme for direct computation of the angular potential with the solution $\mu_*(s)$ of (16).

We consider the following expression for the single-layer potential in the discretization with the approximation

$$\int_{s_j - \frac{h}{2}}^{s_j + \frac{h}{2}} \mu(\sigma) \log |x - y(\sigma)| \, \mathrm{d}\sigma = \frac{1}{2} \int_{s_j - \frac{h}{2}}^{s_j + \frac{h}{2}} \mu(\sigma) \log |x - y(\sigma)|^2 \, \mathrm{d}\sigma. \tag{27}$$

Let $y_r(\sigma) \approx y_r(s_j) + y_r'(s_j)(\sigma - s_j)$, $r = 1, 2$, and $y_r'(s_j)$ can be approximately taken as shown below:

$$y_r'(s_j) \approx \frac{y_r(s_j + h/2) - y_r(s_j - h/2)}{h}, \quad r = 1, 2.$$

We introduce the following notations

$$a_r = x_r - y_r(s_j), \qquad b_r = y_r'(s_j), \qquad r = 1,2,$$
$$c = a_1 b_1 + a_2 b_2, \qquad d^2 = a_1^2 + a_2^2 - c^2 = (a_1 b_2 - a_2 b_1)^2, \qquad d = |a_1 b_2 - a_2 b_1|.$$

Then, using these notations, we obtain

$$\begin{aligned}|x - y(\sigma)|^2 &= (x_1 - y_1(\sigma))^2 + (x_2 - y_2(\sigma))^2 \\ &\approx (x_1 - y_1(s_j) - y_1'(s_j)(\sigma - s_j))^2 + (x_2 - y_2(s_j) - y_2'(s_j)(\sigma - s_j))^2 \\ &= (a_1 - b_1(\sigma - s_j))^2 + (a_2 - b_2(\sigma - s_j))^2 = (\sigma - s_j - c)^2 + d^2,\end{aligned}$$

and, according to our parametrization, we also get $b_1^2 + b_2^2 = 1$.

Hence, passing from μ to μ_* (see(15)) and selecting the singular part in (27), we obtain the following approximation of (27)

$$\int_{s_j-\frac{h}{2}}^{s_j+\frac{h}{2}} \mu(\sigma) \log|x - y(\sigma)|\, \mathrm{d}\sigma \approx \frac{1}{2}\frac{\mu_*(s_j)}{\sqrt{b - s_j}} \int_{s_j-\frac{h}{2}}^{s_j+\frac{h}{2}} \frac{\log((\sigma - s_j - c)^2 + d^2)}{\sqrt{\sigma - a}}\, \mathrm{d}\sigma \tag{28}$$

for the half of the arc close to end point $s = a$. And for the other half of the arc,

$$\int_{s_j-\frac{h}{2}}^{s_j+\frac{h}{2}} \mu(\sigma) \log|x - y(\sigma)|\, \mathrm{d}\sigma \approx \frac{1}{2}\frac{\mu_*(s_j)}{\sqrt{s_j - a}} \int_{s_j-\frac{h}{2}}^{s_j+\frac{h}{2}} \frac{\log((\sigma - s_j - c)^2 + d^2)}{\sqrt{b - \sigma}}\, \mathrm{d}\sigma. \tag{29}$$

Now, let I, and J be the integral parts in (28), and (29), respectively; then we can compute those integrals explicitly such that

$$I = \int_{s_j-\frac{h}{2}}^{s_j+\frac{h}{2}} \frac{\log((\sigma - s_j - c)^2 + d^2)}{\sqrt{\sigma - a}}\, \mathrm{d}\sigma, \qquad s_j - \frac{h}{2} \geq a, \tag{30}$$

$$J = \int_{s_j-\frac{h}{2}}^{s_j+\frac{h}{2}} \frac{\log((\sigma - s_j - c)^2 + d^2)}{\sqrt{b - \sigma}}\, \mathrm{d}\sigma, \qquad s_j + \frac{h}{2} \leq b. \tag{31}$$

After integrating (30) directly, we get

$$\begin{aligned}I = {} & 2\sqrt{\phi + \frac{h}{2}}\, \log\left[\left(c - \frac{h}{2}\right)^2 + d^2\right] - 2\sqrt{\phi - \frac{h}{2}}\, \log\left[\left(c + \frac{h}{2}\right)^2 + d^2\right] \\ & -8I_3\left(\sqrt{\phi + \frac{h}{2}}\right) + 8I_3\left(\sqrt{\phi - \frac{h}{2}}\right), \qquad \text{for } d \neq 0,\end{aligned}$$

where $I_3(\xi) = \xi + \dfrac{p}{8}\log\dfrac{\xi^2 - p\xi + q}{\xi^2 + p\xi + q} - m\left(\arctan\dfrac{2\xi + p}{4m} + \arctan\dfrac{2\xi - p}{4m}\right)$,

$\phi = s_j - a,\ g = \phi + c,\ q = \sqrt{g^2 + d^2},\ p = \sqrt{2(q + g)},\ m = \dfrac{1}{2}\sqrt{\dfrac{q - g}{2}}$.

And similarly, we get

$$\begin{aligned}J = {} & 2\sqrt{\kappa + \frac{h}{2}}\, \log\left[\left(c + \frac{h}{2}\right)^2 + d^2\right] - 2\sqrt{\kappa - \frac{h}{2}}\, \log\left[\left(c - \frac{h}{2}\right)^2 + d^2\right] \\ & +8J_3\left(\sqrt{\kappa - \frac{h}{2}}\right) - 8J_3\left(\sqrt{\kappa + \frac{h}{2}}\right), \qquad \text{for } d \neq 0,\end{aligned}$$

where $J_3(\zeta) = \zeta + \dfrac{\tilde{p}}{8}\log\dfrac{\zeta^2 - \tilde{p}\zeta + \tilde{q}}{\zeta^2 + \tilde{p}\zeta + \tilde{q}} - \tilde{m}\left(\arctan\dfrac{2\zeta + \tilde{p}}{4\tilde{m}} + \arctan\dfrac{2\zeta - \tilde{p}}{4\tilde{m}}\right)$,

$\kappa = b - s_j,\ l = \kappa - c,\ \tilde{q} = \sqrt{l^2 + d^2},\ \tilde{p} = \sqrt{2(\tilde{q} + l)},\ \tilde{m} = \dfrac{1}{2}\sqrt{\dfrac{\tilde{q} - l}{2}}$.

For the case of $d = 0$, I and J are as below:

$$I = \begin{cases} 2\sqrt{\phi + \frac{h}{2}} \log\left[\left(c - \frac{h}{2}\right)^2\right] - 2\sqrt{\phi - \frac{h}{2}} \log\left[\left(c + \frac{h}{2}\right)^2\right] \\ -8\left(\sqrt{\phi + \frac{h}{2}} - \sqrt{\phi - \frac{h}{2}} + \frac{1}{2}\sqrt{g} \log\left|\frac{\left(\sqrt{\phi + \frac{h}{2}} - \sqrt{g}\right)\left(\sqrt{\phi - \frac{h}{2}} + \sqrt{g}\right)}{\left(\sqrt{\phi + \frac{h}{2}} + \sqrt{g}\right)\left(\sqrt{\phi - \frac{h}{2}} - \sqrt{g}\right)}\right|\right) \\ \text{if } g \geq 0, \\ 2\sqrt{\phi + \frac{h}{2}} \log\left[\left(c - \frac{h}{2}\right)^2\right] - 2\sqrt{\phi - \frac{h}{2}} \log\left[\left(c + \frac{h}{2}\right)^2\right] \\ -8\left(\sqrt{\phi + \frac{h}{2}} - \sqrt{\phi - \frac{h}{2}} - \sqrt{-g}\left(\arctan\left(\frac{\sqrt{\phi + \frac{h}{2}}}{\sqrt{-g}}\right) - \arctan\left(\frac{\sqrt{\phi - \frac{h}{2}}}{\sqrt{-g}}\right)\right)\right) \\ \text{if } g < 0, \end{cases}$$

where $c \neq \frac{h}{2}$ and $c \neq -\frac{h}{2}$.

$$J = \begin{cases} 2\sqrt{\kappa + \frac{h}{2}} \log\left[\left(c + \frac{h}{2}\right)^2\right] - 2\sqrt{\kappa - \frac{h}{2}} \log\left[\left(c - \frac{h}{2}\right)^2\right] \\ -8\left(\sqrt{\kappa + \frac{h}{2}} - \sqrt{\kappa - \frac{h}{2}} + \frac{1}{2}\sqrt{l} \log\left|\frac{\left(\sqrt{\kappa + \frac{h}{2}} - \sqrt{l}\right)\left(\sqrt{\kappa - \frac{h}{2}} + \sqrt{l}\right)}{\left(\sqrt{\kappa + \frac{h}{2}} + \sqrt{l}\right)\left(\sqrt{\kappa - \frac{h}{2}} - \sqrt{l}\right)}\right|\right) \\ \text{if } l \geq 0, \\ 2\sqrt{\kappa + \frac{h}{2}} \log\left[\left(c + \frac{h}{2}\right)^2\right] - 2\sqrt{\kappa - \frac{h}{2}} \log\left[\left(c - \frac{h}{2}\right)^2\right] \\ -8\left(\sqrt{\kappa + \frac{h}{2}} - \sqrt{\kappa - \frac{h}{2}} - \sqrt{-l}\left(\arctan\left(\frac{\sqrt{\kappa + \frac{h}{2}}}{\sqrt{-l}}\right) - \arctan\left(\frac{\sqrt{\kappa - \frac{h}{2}}}{\sqrt{-l}}\right)\right)\right) \\ \text{if } l < 0, \end{cases}$$

where $c \neq \frac{h}{2}$ and $c \neq -\frac{h}{2}$ (see the Appendix for details of the derivations).

Now we present results of the evaluation of the integrals I and J in special cases, when $d = 0$ and $c = \pm h/2$.

Consider special cases for the integral I. If $d = 0$, $c = h/2$ and $g = \phi + c > 0$, we have

$$I = 8\sqrt{\phi + h/2} \log\left|2\sqrt{\phi + h/2}\right| - 4\left(\sqrt{\phi - h/2} - \sqrt{\phi + h/2}\right) \log h \\ -8\sqrt{\phi + h/2} \log\left|\sqrt{\phi - h/2} + \sqrt{\phi + h/2}\right| + 8\left(\sqrt{\phi - h/2} - \sqrt{\phi + h/2}\right).$$

If $d = 0,\ \ c = -h/2$ and $g = \phi + c > 0$, then

$$I = 4\left(\sqrt{\phi + h/2} - \sqrt{\phi - h/2}\right)\log h + 8\sqrt{\phi - h/2}\,\log\left|\sqrt{\phi + h/2} + \sqrt{\phi - h/2}\right| - 8\sqrt{\phi - h/2}\log\left|2\sqrt{\phi - h/2}\right| + 8\left(\sqrt{\phi - h/2} - \sqrt{\phi + h/2}\right).$$

If $d = 0,\ \ c = -h/2$ and $g = \phi + c = 0$, then $\ I = 4\sqrt{h}\,\log h - 8\sqrt{h}$.

Consider special cases for the integral J. If $d = 0,\ \ c = h/2$ and $l = \kappa - c > 0$, we have

$$J = -8\sqrt{\kappa - h/2}\,\log\left|2\sqrt{\kappa - h/2}\right| - 4\left(\sqrt{\kappa - h/2} - \sqrt{\kappa + h/2}\right)\log h + 8\sqrt{\kappa - h/2}\,\log\left|\sqrt{\kappa + h/2} + \sqrt{\kappa - h/2}\right| + 8\left(\sqrt{\kappa - h/2} - \sqrt{\kappa + h/2}\right).$$

If $d = 0,\ \ c = -h/2$ and $l = \kappa - c > 0$, then

$$J = 4\left(\sqrt{\kappa + h/2} - \sqrt{\kappa - h/2}\right)\log h - 8\sqrt{\kappa + h/2}\,\log\left|\sqrt{\kappa - h/2} + \sqrt{\kappa + h/2}\right| + 8\sqrt{\kappa + h/2}\log\left|2\sqrt{\kappa + h/2}\right| + 8\left(\sqrt{\kappa - h/2} - \sqrt{\kappa + h/2}\right).$$

If $d = 0,\ \ c = h/2$ and $l = \kappa - c = 0$, then $\ J = 4\sqrt{h}\,\log h - 8\sqrt{h}$.

Thus, explicit formulas for the integrals I and J are presented for all cases.

So, to compute the single-layer potential, we modify formula (10) to (28), (29), select the singular part of the integrand and evaluate the integral with the singular part explicitly. We call this scheme "selection of singularity".

Now, we consider the formula (5) for recovery of the angular potential. For this, we have to compute the kernel $V(x,s)$ which satisfies the relations (6). Hence, we should take any fixed branch of the kernel $V(x,s)$, which changes continuously in s along Γ for a given fixed x outside Γ. We suggest the following procedure with the pseudo-code concept for the computation of the kernel $V(x,s)$.

Let $s_1 = a + h/2$, compute $\sin(\bar{V}(x,s_1)) = \dfrac{x_2 - y_2(s_1)}{|x - y(s_1)|}$ and put

$$V(x,s_1) = \begin{cases} \arccos\left(\dfrac{x_1 - y_1(s_1)}{|x - y(s_1)|}\right) + \text{add}, & \text{if } \sin(\bar{V}(x,s_1)) > 0, \\ -\arccos\left(\dfrac{x_1 - y_1(s_1)}{|x - y(s_1)|}\right) + \text{add}, & \text{if } \sin(\bar{V}(x,s_1)) < 0, \end{cases} \tag{32}$$

where add $= 0$ initially.

Assume that $V(x,s_{k-1})$ is known and then find $V(x,s_k)$:

If $\sin(\bar{V}(x,s_k)) = \dfrac{x_2 - y_2(s_k)}{|x - y(s_k)|} > 0$, put $\bar{V}(x,s_k) = \arccos\left(\dfrac{x_1 - y_1(s_k)}{|x - y(s_k)|}\right) + \text{add}$, in addition, if inequality

$$\bar{V}(x,s_k) - V(x,s_{k-1}) > \pi, \tag{33}$$

is true, then put add $= -2\pi + \text{add}$ and $V(x,s_k) = \arccos\left(\dfrac{x_1 - y_1(s_k)}{|x - y(s_k)|}\right) + \text{add}$; while if inequality (33) is not true, then put $V(x,s_k) = \bar{V}(x,s_k)$.

If $\sin(\bar{V}(x,s_k)) = \dfrac{x_2 - y_2(s_k)}{|x - y(s_k)|} < 0$, put $\bar{V}(x,s_k) = -\arccos\left(\dfrac{x_1 - y_1(s_k)}{|x - y(s_k)|}\right) + \text{add}$, in addition, if inequality

$$\bar{V}(x,s_k) - V(x,s_{k-1}) < -\pi, \tag{34}$$

is true, then put add $= 2\pi + \text{add}$ and $V(x,s_k) = -\arccos\left(\dfrac{x_1 - y_1(s_k)}{|x - y(s_k)|}\right) + \text{add}$; while, if inequality (34) is not true, then put $V(x,s_k) = \bar{V}(x,s_k)$. This procedure allows us to compute the continuous kernel $V(x,s)$

directly using mathematical induction. The code for the computation of the kernel $V(x,s)$ is given in Sect. A.4 of the Appendix.

Now we can get the angular potential

$$\begin{aligned}\nu[\mu](x) &= -\frac{1}{2\pi}\int_a^b \mu(\sigma)\, V(x,\sigma)\mathrm{d}\sigma \\ &= -\frac{1}{2\pi}\int_a^b \frac{\mu_*(\sigma)}{\sqrt{\sigma-a}\sqrt{b-\sigma}}\, V(x,\sigma)\mathrm{d}\sigma \\ &\approx -\frac{1}{2\pi}\left[\frac{\mu_*(s_1)}{\sqrt{b-s_1}}2\sqrt{h}\, V(x,s_1) + \frac{\mu_*(s_M)}{\sqrt{s_M-a}}2\sqrt{h}\, V(x,s_M) + \sum_{k=2}^{M-1}\frac{\mu_*(s_k)\, V(x,s_k)h}{\sqrt{s_k-a}\sqrt{b-s_k}}\right] \end{aligned} \tag{35}$$

with a continuous branch of the kernel $V(x,s_k)$ for each discretization step, $k = 1,2,\ldots,M$. In deriving (35) we have used (22), (23), (24).

To get a more efficient computation of $\nu[\mu](x)$, we consider the integral of the singular part

$$\int_{s_k-h/2}^{s_k+h/2}\frac{1}{\sqrt{b-\sigma}\sqrt{\sigma-a}}\,\mathrm{d}\sigma = \int_{s_k-h/2}^{s_k+h/2}\frac{1}{\sqrt{-ab+(a+b)\sigma-\sigma^2}}\,\mathrm{d}\sigma,$$

as a modification of (21), (35).

Let $\gamma_1 = -ab$, $\gamma_2 = a+b$, and $\gamma_3 = -1$, then

$$\begin{aligned}\int_{s_k-h/2}^{s_k+h/2}\frac{1}{\sqrt{\gamma_1+\gamma_2\sigma+\gamma_3\sigma^2}}\,\mathrm{d}\sigma &= \frac{-1}{\sqrt{-\gamma_3}}\arcsin\frac{2\gamma_3\sigma+\gamma_2}{\sqrt{\gamma_2^2-4\gamma_1\gamma_3}}\Bigg|_{s_k-h/2}^{s_k+h/2} \\ &= \frac{-1}{\sqrt{1}}\arcsin\frac{2(-1)\sigma+(a+b)}{\sqrt{(a+b)^2-4(-ab)(-1)}}\Bigg|_{s_k-h/2}^{s_k+h/2} \\ &= \arcsin\frac{2\sigma-(b+a)}{b-a}\Bigg|_{s_k-h/2}^{s_k+h/2}.\end{aligned}$$

Hence, we get a modified recovery formula for the angular potential $\nu[\mu](x)$ with kernel $V(x,s)$ as follows:

$$\begin{aligned}\nu[\mu](x) &= -\frac{1}{2\pi}\int_a^b \frac{\mu_*(\sigma)}{\sqrt{\sigma-a}\sqrt{b-\sigma}}\, V(x,\sigma)\mathrm{d}\sigma \\ &\approx -\frac{1}{2\pi}\sum_{k=1}^{M}\mu_*(s_k)V(x,s_k)\arcsin\frac{2\sigma-(b+a)}{b-a}\Bigg|_{s_k-h/2}^{s_k+h/2}.\end{aligned} \tag{36}$$

The numerical scheme based on (36) is called the "direct computation" scheme for the angular potential.

In the recovery of the angular potential, if the distance from x to the arc Γ, that is $\min\limits_{\sigma\in[a,b]}|x-y(\sigma)|$, is sufficiently small, then the absolute value of the angular kernel changes too fast when $y(s)$ moves along the part of Γ nearest to x. Therefore the accuracy of the angular potential decays near the arc. To improve the accuracy near the arc, we subdivide once more each interval of length h into M_1 sub-intervals with uniform step size $h_1 = \frac{h}{M_1}$. The values of μ_* on the subintervals are computed by interpolation of three μ_*-values near the interval $[s_k-\frac{h}{2}, s_k+\frac{h}{2}]$, that is

$$\begin{aligned}\mu_*(\xi) &= \mu_*(s_k) + \frac{\mu_*(s_{k+1})-\mu_*(s_{k-1})}{2h}(\xi-s_k) \\ &\quad + \frac{\mu_*(s_{k+1})+\mu_*(s_{k-1})-2\mu_*(s_k)}{h^2}\,\frac{(\xi-s_k)^2}{2},\end{aligned}$$

for $\xi\in[s_k-\frac{h}{2}, s_k+\frac{h}{2}]$. This remedial scheme for the angular potential is called "subdivision scheme".

6 Numerical tests and accuracy of the method

The construction of the numerical solution of problem 2.1 consists of two steps. The first step is the numerical solution of integral equation (16) according to Sect. 4. The second step is the numerical computation of the potentials according to Sect. 5. Hence, our tests are divided into two parts as well. The aim of the first set of tests is to check our method proposed in Sect. 4 for numerically solving integral equation (16), while the second set of tests is devoted to testing the numerical method proposed in Sect. 5 for the computation of the potentials.

To check the numerical method proposed in Sect. 4 for solving Eq. (16), we consider the numerical tests for the intercept and for an open arc on the unit circle. For the numerical tests, we obtain an exact analytical solution μ_* of Eq. (16) in these particular cases (intercept and arc of a circle).

First, if Γ is an intercept of the straight line:

$$x_1(s) = s\cos\alpha, \quad x_2(s) = s\sin\alpha, \quad \alpha = \text{const}, \quad s \in [a,b],$$

then $Y(s,\sigma) \equiv 0$, $A(s,\sigma) \equiv 0$, and the functions

$$\mu(s) = \frac{1}{\sqrt{s-a}\sqrt{b-s}}\Phi(s), \qquad \mu_*(s) = \Phi(s) \tag{37}$$

are solutions of Eqs. (14) and (16), respectively. Additionally, if $f(s) = c_1$, where c_1 is an arbitrary constant, then

$$\Phi(s) = \frac{2c_1}{1+\beta^2} I_0(s) = \frac{2c_1}{1+\beta^2}\left(\frac{a+b}{2} - s\right), \tag{38}$$

in accordance with (18), (19).

Second, if Γ is an arc of the unit circle, $s = \theta_0$ is a polar angle, and a, b are polar angles of the end-points of Γ, then the solution of the system of Eqs. (7), (11) is

$$\mu(\theta_0) = \frac{1}{\pi(1+\beta^2)R_1(\theta_0)} \int_a^b \frac{R_1(\theta) f(\theta)}{\sin\frac{\theta-\theta_0}{2}} \mathrm{d}\theta, \tag{39}$$

where $\theta_0 = s \in [a,b]$ and

$$R_1(\theta) = 2\left(\sin\frac{\theta-a}{2}\right)^{\frac{1}{2}}\left(\sin\frac{b-\theta}{2}\right)^{\frac{1}{2}}, \text{(positive root)}.$$

The derivation of (39) is presented in the Appendix. Note that system (7), (11) is equivalent to Eq. (14). Using (39) we obtain a solution of Eq. (16) by the formula

$$\mu_*(\theta_0) = \mu(\theta_0)\sqrt{\theta_0 - a}\sqrt{b-\theta_0}, \qquad \theta_0 \in [a,b]. \tag{40}$$

If $f(\theta) \equiv c_2$, where c_2 is an arbitrary constant, then, evaluating integral in (39), we obtain

$$\mu(\theta_0) = 4\frac{c_2}{R_1(\theta_0)} \sin\left(\frac{a+b}{4} - \frac{\theta_0}{2}\right)\frac{1}{1+\beta^2}. \tag{41}$$

If $f(\theta) \equiv A\cos\theta + B\sin\theta$, where A and B are constants, then from (39) we get

$$\begin{aligned}\mu(\theta_0) &= \frac{1}{\pi(1+\beta^2)R_1(\theta_0)} \int_a^b \frac{R_1(\theta) f(\theta)}{\sin\frac{\theta-\theta_0}{2}} \mathrm{d}\theta \\ &= \frac{2}{(1+\beta^2)R_1(\theta_0)}\left[A\left\{\sin\left(\frac{\theta_0}{2} + \frac{a+b}{4}\right)\cos\frac{a-b}{2} - \sin\left(\frac{3}{2}\theta_0 - \frac{a+b}{4}\right)\right\}\right. \\ &\quad \left. + B\left\{\cos\left(\frac{3}{2}\theta_0 - \frac{a+b}{4}\right) - \cos\left(\frac{\theta_0}{2} + \frac{a+b}{4}\right)\cos\frac{a-b}{2}\right\}\right].\end{aligned} \tag{42}$$

The formulae (41) and (42) are derived from (39) in the Appendix. Substituting (41) or (42) in (40), we obtain a solution of Eq. (16) on the arc Γ of the unit circle when $f(\theta) \equiv c_2$ or when $f(\theta) \equiv A\cos\theta + B\sin\theta$, respectively.

We now consider the tests devoted to checking the numerical schemes presented in Sect. 5 for the computation of the potentials. For these tests we obtain exact analytical expressions for the potentials on the intercept of a straight line and on the arc of the unit circle in certain cases. First we derive exact analytical expressions for the potentials defined at the intercept of a straight line for the case when the integrals in the potentials can be evaluated analytically.

Let Γ be taken along the x_1-axis such that $a = -1,\ b = 1,\ -1 \le s \le 1$, i.e.,

$$\Gamma = \{x = (x_1, x_2) | \, x_2 = 0,\ x_1 = s,\ -1 \le s \le 1\}.$$

In this case problem 2.1 with $f \equiv 1$ has an exact analytical solution, which is derived below. In doing so, integrals in the angular potential from (5) and in the single-layer potential from (10) are evaluated analytically. From the formulas (37), (38) with $f \equiv 1$, we have the following exact solution of integral equation (14):

$$\mu(s) = \frac{2}{1+\beta^2}\left(\frac{a+b}{2} - s\right)\frac{1}{\sqrt{1-s^2}} = \frac{2}{1+\beta^2}\left(-\frac{s}{\sqrt{1-s^2}}\right). \tag{43}$$

Consider

$$\rho(s) = \int_{-1}^{s} \mu(\sigma)\mathrm{d}\sigma = \frac{-2}{1+\beta^2}\int_{-1}^{s}\frac{\sigma}{\sqrt{1-\sigma^2}}\mathrm{d}\sigma = \frac{2}{1+\beta^2}\sqrt{1-s^2}.$$

Setting $z = x_1 + \mathrm{i}x_2,\ \tilde{y} = y_1 + \mathrm{i}y_2$, introduce the function

$$\begin{aligned} F(z) &= w[\mu](x) + \mathrm{i}v[\mu](x) \\ &= -\frac{1}{2\pi}\int_a^b \mu(t)\log(z - \tilde{y}(t))\mathrm{d}t \\ &= -\frac{1}{2\pi}\int_a^b \log(z-\tilde{y}(t))\mathrm{d}\rho(t) \\ &= -\frac{1}{2\pi}\rho(t)\log(z-\tilde{y}(t))\ \Big|_a^b + \frac{1}{2\pi}\int_a^b \frac{\rho(t)}{\tilde{y}(t)-z}\tilde{y}'(t)\mathrm{d}t \\ &= \frac{1}{2\pi}\int_a^b \frac{\rho(t)}{\tilde{y}(t)-z}\tilde{y}'(t)\mathrm{d}t \end{aligned}$$

because $\rho(a) = \rho(b) = 0$. Since $y(t) = (t, 0),\ \tilde{y}(t) = t,\ \tilde{y}(t) - z = t - z$, and $\tilde{y}'(t) = 1$, we obtain

$$F(z) = \frac{1}{\pi(1+\beta^2)}\int_{-1}^{1}\frac{\sqrt{1-t^2}}{t-z}\mathrm{d}t.$$

Now, we can evaluate this integral for $z \notin \Gamma$. According to Plemelj's formulas [10, Sect. 16] we obtain on Γ:

$$F^+(t) - F^-(t) = 2\mathrm{i}(1+\beta^2)^{-1}\sqrt{1-t^2},$$

where the limit values of $F(z)$ on Γ^+ and Γ^- are denoted by $F^+(t)$ and $F^-(t)$, respectively.

Consider the function $\sqrt{z^2-1}$ which is analytic outside Γ and

$$\sqrt{z^2-1}\ \Big|_{z\to t\in\Gamma^{\pm}} = \pm\mathrm{i}\sqrt{1-t^2}.$$

If $z \to \infty$, then

$$\sqrt{z^2-1} = z\left(1-\frac{1}{z^2}\right)^{\frac{1}{2}} \approx z\left(1-\frac{1}{2z^2}\right) \approx z + O(z^{-1}).$$

Clearly, the function $(\sqrt{z^2-1}-z)$ tends to zero as $z\to\infty$. Consequently, both the function $F(z)$ and the function $(1+\beta^2)^{-1}(\sqrt{z^2-1}-z)$ satisfy the same jump problem formulated below.

Jump problem: Find a piecewise-holomorphic function $F(z)$ with line of jumps Γ, so that $F(\infty)=0$ and $F(z)$ satisfies the boundary condition on Γ:

$$F^+(t)-F^-(t)=2\mathrm{i}(1+\beta^2)^{-1}\sqrt{1-t^2}.$$

Since the solution of this jump problem is unique [10, Sect. 31], we obtain

$$F(z)=(1+\beta^2)^{-1}(\sqrt{z^2-1}-z).$$

Thus, the integral $F(z)$ is evaluated.

We can take polar coordinates in the points $a=-1$, and $b=1$ such that

$$z-a=r_1\mathrm{e}^{\mathrm{i}\varphi_1},\quad z-b=r_2\mathrm{e}^{\mathrm{i}\varphi_2}$$

where $r_1=\sqrt{(x_1-a)^2+x_2^2}$, $r_2=\sqrt{(x_1-b)^2+x_2^2}$. Hence

$$\cos\varphi_1=\frac{x_1-a}{r_1},\qquad \sin\varphi_1=\frac{x_2}{r_1},$$
$$\cos\varphi_2=\frac{x_1-b}{r_2},\qquad \sin\varphi_2=\frac{x_2}{r_2}.$$

Therefore for $x_2\neq 0$: $\varphi_1=\mathrm{sgn}(x_2)\arccos\dfrac{x_1-a}{r_1}$, $\varphi_2=\mathrm{sgn}(x_2)\arccos\dfrac{x_1-b}{r_2}$. Then

$$q(z)=\sqrt{z-a}\sqrt{z-b}=\sqrt{r_1r_2}\mathrm{e}^{\mathrm{i}\frac{\varphi_1}{2}}\mathrm{e}^{\mathrm{i}\frac{\varphi_2}{2}},$$

and

$$\mathfrak{Re}\,q(z)=\sqrt{r_1r_2}\left\{\cos\frac{\varphi_1}{2}\cos\frac{\varphi_2}{2}-\sin\frac{\varphi_1}{2}\sin\frac{\varphi_2}{2}\right\},$$
$$\mathfrak{Im}\,q(z)=\sqrt{r_1r_2}\left\{\cos\frac{\varphi_1}{2}\sin\frac{\varphi_2}{2}+\cos\frac{\varphi_2}{2}\sin\frac{\varphi_1}{2}\right\}.$$

Consequently,

$$w[\mu](x)=\mathfrak{Re}\,F(z)=\frac{1}{(1+\beta^2)}\{\mathfrak{Re}\,q(z)-x_1\},\tag{44}$$
$$v[\mu](x)=\mathfrak{Im}\,F(z)=\frac{1}{(1+\beta^2)}\{\mathfrak{Im}\,q(z)-x_2\}.\tag{45}$$

With (44) and (45), finally, we get the solution $u(x)$ of the problem 2.1 by the formula (9). This is an explicit solution of the problem 2.1 with $f\equiv 1$ if Γ is an intercept $[-1,1]$ on the Ox_1-axis.

Now, we obtain the exact analytical expressions for potentials defined on the arc of the unit circle.

Let Γ be an arc of the unit circle, $-b<\theta<b$, θ is a polar angle, the constant $b\in(0,\pi)$. The single layer potential is

$$w[\mu](x)=-\frac{1}{2\pi}\int_{-b}^{b}\mu(\theta)\log\sqrt{(x_1-\cos(\theta))^2+(x_2-\sin(\theta))^2}\mathrm{d}\theta,$$

while the angular potential is

$$v[\mu](x)=-\frac{1}{2\pi}\int_{-b}^{b}\mu(\theta)V(x,\theta)\mathrm{d}\theta,$$

where $V(x,\theta)$ is the kernel of the angular potential.

Let $\Psi_0(z)$ be

$$\Psi_0(z) = \frac{1}{2}\left(\sqrt{z-\mathrm{e}^{-\mathrm{i}b}}\sqrt{z-\mathrm{e}^{\mathrm{i}b}} + \frac{\mathrm{e}^{-\mathrm{i}b}+\mathrm{e}^{\mathrm{i}b}}{2} - z\right) \tag{46}$$

and $\Psi_0(z)$ is analytic outside Γ. Note that $\Psi_0(\infty) = 0$, and the following relationship holds on Γ

$$\Psi_0^+(t) - \Psi_0^-(t) = (\sqrt{t-\mathrm{e}^{-\mathrm{i}b}}\sqrt{t-\mathrm{e}^{\mathrm{i}b}})|_{\Gamma^+} = \sqrt{t-\mathrm{e}^{-\mathrm{i}b}}\sqrt{t-\mathrm{e}^{\mathrm{i}b}} = q_0(t), \quad t \in \Gamma, \tag{47}$$

where limit values of functions on Γ^+ and Γ^- are denoted by the superscripts $+$ and $-$, respectively. Therefore $\Psi_0(z)$ is a solution of the following jump problem.

Jump problem: Find a piecewise holomorphic function $\Psi_0(z)$ with the line of jumps Γ satisfying the boundary condition: $\Psi_0^+(t_0) - \Psi_0^-(t_0) = q_0(t_0)$ on Γ and such that $\Psi_0(\infty) = 0$.

One can show [10, Sect. 31] that the solution of this jump problem is unique. So, $\Psi_0(z)$ is the unique solution of the jump problem. Using Plemelj formulas [10, Sect. 16], we obtain a new integral representation for the solution of the jump problem in the following form

$$\begin{aligned}
\Psi_0(z) &= \frac{1}{2\pi\mathrm{i}}\int_\Gamma \frac{q_0(t)}{t-z}\,\mathrm{d}t \\
&= \frac{1}{2\pi\mathrm{i}}\int_\Gamma q_0(t)\,\mathrm{d}(\log|t-z| + \mathrm{i}\arg(t-z)) \\
&= \frac{1}{2\pi\mathrm{i}} q_0(t)\left\{\log|t-z| + \mathrm{i}\arg(t-z)\right\}\Big|_{\mathrm{e}^{-\mathrm{i}b}}^{\mathrm{e}^{\mathrm{i}b}} \\
&\quad -\frac{1}{2\pi\mathrm{i}}\int_\Gamma q_0'(t)\left\{\log|t-z| + \mathrm{i}\arg(t-z)\right\}\mathrm{d}t \\
&= -\frac{1}{2\pi\mathrm{i}}\int_\Gamma q_0'(t)(\log|z-t| + \mathrm{i}\arg(z-t))\,\mathrm{d}t,
\end{aligned} \tag{48}$$

where $q_0(t)$ is given by (47) and so

$$q_0'(t) = \frac{2t-\mathrm{e}^{-\mathrm{i}b}-\mathrm{e}^{\mathrm{i}b}}{2\sqrt{t-\mathrm{e}^{-\mathrm{i}b}}\sqrt{t-\mathrm{e}^{\mathrm{i}b}}}.$$

In deriving (48) we used the following relationships: $\arg(t-z) = \arg(z-t) + \pi\,\mathrm{i}$ and

$$\int_\Gamma q_0'(t)\,\mathrm{d}t = 0.$$

To get another form of $q_0'(t)$, set $t = \mathrm{e}^{\mathrm{i}\theta}$; then

$$\begin{aligned}
\sqrt{t-\mathrm{e}^{-\mathrm{i}b}}\sqrt{t-\mathrm{e}^{\mathrm{i}b}} &= \sqrt{\mathrm{e}^{\mathrm{i}\theta}-\mathrm{e}^{-\mathrm{i}b}}\sqrt{\mathrm{e}^{\mathrm{i}\theta}-\mathrm{e}^{\mathrm{i}b}} \\
&= 2\sqrt{\mathrm{e}^{\mathrm{i}\left(\frac{\pi}{2}+\frac{\theta-b}{2}\right)}\sin\frac{\theta+b}{2}}\sqrt{\mathrm{e}^{\mathrm{i}\left(\frac{\pi}{2}+\frac{\theta+b}{2}\right)}\sin\frac{\theta-b}{2}} \\
&= 2\sqrt{\sin\frac{\theta+b}{2}}\sqrt{\sin\frac{\theta-b}{2}}\,\mathrm{e}^{\mathrm{i}\left(\frac{\pi}{2}+\frac{\theta}{2}\right)} \\
&= \mathrm{i}2\sqrt{\sin\frac{\theta+b}{2}}\sqrt{\sin\frac{\theta-b}{2}}\,\mathrm{e}^{\mathrm{i}\frac{\theta}{2}} \\
&= -2\sqrt{\sin\frac{\theta+b}{2}}\sqrt{\sin\frac{b-\theta}{2}}\,\mathrm{e}^{\mathrm{i}\frac{\theta}{2}}.
\end{aligned}$$

Hence,

$$q_0'(t) = \frac{2\mathrm{e}^{\mathrm{i}\theta}-\mathrm{e}^{-\mathrm{i}b}-\mathrm{e}^{\mathrm{i}b}}{2\left(-2\sqrt{\sin\frac{\theta+b}{2}}\sqrt{\sin\frac{b-\theta}{2}}\,\mathrm{e}^{\mathrm{i}\frac{\theta}{2}}\right)} = \frac{\left(\cos b-\mathrm{e}^{\mathrm{i}\theta}\right)\mathrm{e}^{-\mathrm{i}\frac{\theta}{2}}}{\left(2\sqrt{\sin\frac{\theta+b}{2}}\sqrt{\sin\frac{b-\theta}{2}}\right)}. \tag{49}$$

Therefore, $q_0'(t)$ in (48) can be replaced by (49), so that

$$\begin{aligned}\Psi_0(z) &= -\frac{1}{2\pi \mathrm{i}} \int_\Gamma \frac{\left(\cos b - \mathrm{e}^{\mathrm{i}\theta}\right) \mathrm{e}^{-\mathrm{i}\frac{\theta}{2}}}{\left(2\sqrt{\sin\frac{\theta+b}{2}}\sqrt{\sin\frac{b-\theta}{2}}\right)} \left\{\log|z-t| + \mathrm{i}\arg(z-t)\right\} \mathrm{d}t \\ &= -\frac{1}{2\pi \mathrm{i}} \int_{-b}^{b} \frac{\left(\cos b - \mathrm{e}^{\mathrm{i}\theta}\right) \mathrm{e}^{-\mathrm{i}\frac{\theta}{2}}}{R_0(\theta)} \left\{\log|z-t| + \mathrm{i}\arg(z-t)\right\} \mathrm{i}\mathrm{e}^{\mathrm{i}\theta} \,\mathrm{d}\theta \\ &= -\frac{1}{2\pi} \int_{-b}^{b} \frac{\left(\mathrm{e}^{\mathrm{i}\frac{\theta}{2}} \cos b - \mathrm{e}^{\mathrm{i}\frac{3\theta}{2}}\right)}{R_0(\theta)} \left\{\log|z-t| + \mathrm{i}\arg(z-t)\right\} \mathrm{d}\theta, \end{aligned} \tag{50}$$

where $\mathrm{d}t = \mathrm{i}\mathrm{e}^{\mathrm{i}\theta}\mathrm{d}\theta$, and $R_0(\theta) = 2\sqrt{\sin\dfrac{\theta+b}{2}}\sqrt{\sin\dfrac{b-\theta}{2}}$.

Set $\mu_1(\theta) = \dfrac{\cos\frac{\theta}{2}\cos b - \cos\frac{3\theta}{2}}{R_0(\theta)}$, $\quad \mu_2(\theta) = \dfrac{\sin\frac{\theta}{2}\cos b - \sin\frac{3\theta}{2}}{R_0(\theta)}$. From (46), and (50), we get

$$\begin{aligned}\mathfrak{Re}(\Psi_0(z)) &= \mathfrak{Re}\left[\frac{1}{2}(\sqrt{z-\mathrm{e}^{-\mathrm{i}b}}\sqrt{z-\mathrm{e}^{\mathrm{i}b}} + \frac{\mathrm{e}^{-\mathrm{i}b}+\mathrm{e}^{\mathrm{i}b}}{2} - z)\right] \\ &= -\frac{1}{2\pi}\mathfrak{Re}\left[\int_{-b}^{b} (\mu_1(\theta) + \mathrm{i}\mu_2(\theta)) \left\{\log|z-t| + \mathrm{i}\arg(z-t)\right\} \mathrm{d}\theta\right] \\ &= -\frac{1}{2\pi}\int_{-b}^{b} \left[\mu_1(\theta)\log|z-t| - \mu_2(\theta)\arg(z-t)\right] \mathrm{d}\theta \\ &= w[\mu_1](x) - v[\mu_2](x), \end{aligned} \tag{51}$$

and

$$\begin{aligned}\mathfrak{Im}(\Psi_0(z)) &= \mathfrak{Im}\left[\frac{1}{2}(\sqrt{z-\mathrm{e}^{-\mathrm{i}b}}\sqrt{z-\mathrm{e}^{\mathrm{i}b}} + \frac{\mathrm{e}^{-\mathrm{i}b}+\mathrm{e}^{\mathrm{i}b}}{2} - z)\right] \\ &= -\frac{1}{2\pi}\mathfrak{Im}\left[\int_{-b}^{b} (\mu_1(\theta) + \mathrm{i}\mu_2(\theta)) \left\{\log|z-t| + \mathrm{i}\arg(z-t)\right\} \mathrm{d}\theta\right] \\ &= -\frac{1}{2\pi}\int_{-b}^{b} \left[\mu_2(\theta)\log|z-t| + \mu_1(\theta)\arg(z-t)\right] \mathrm{d}\theta \\ &= w[\mu_2](x) + v[\mu_1](x), \end{aligned} \tag{52}$$

where $x = (x_1, x_2)$, and $z = x_1 + \mathrm{i}x_2$.

Finally, we obtain the following relationships from (51) and (52) for any x outside Γ:

$$\left| w[\mu_1](x) - v[\mu_2](x) - \frac{\cos b}{2} + \frac{x_1}{2} \right| = \frac{\left|\mathfrak{Re}\left(\sqrt{z-\mathrm{e}^{-\mathrm{i}b}}\sqrt{z-\mathrm{e}^{\mathrm{i}b}}\right)\right|}{2}, \tag{53}$$

$$\left| w[\mu_2](x) + v[\mu_1](x) + \frac{x_2}{2} \right| = \frac{\left|\mathfrak{Im}\left(\sqrt{z-\mathrm{e}^{-\mathrm{i}b}}\sqrt{z-\mathrm{e}^{\mathrm{i}b}}\right)\right|}{2}. \tag{54}$$

The equalities (53) and (54) allow us to check the selection-of-singularity formulae for the single-layer potential and to check the subdivisions algorithm for the angular potential, if the density in the potentials has square-root singularities at the ends of Γ. Besides, there are useful equalities for these tests,

$$w[\mu_1](x^0) - v[\mu_2](x^0) - \frac{1}{2}\cos b = -\frac{1}{2}, \qquad w[\mu_2](x^0) + v[\mu_1](x^0) = 0,$$

where $x^0 = (0,0)$, i.e., $x_1^0 = x_2^0 = 0$.

In the next subsections, we describe the results of the numerical tests mentioned above. In the result tables, we present the L^2-error and relative errors between the analytical solutions $\mu_*(x)$, $w[\mu](x)$, $v[\mu](x)$, and related numerical solutions $\tilde{\mu}_*(x)$, $\tilde{w}[\mu](x)$, $\tilde{v}[\mu](x)$, which are denoted by a tilde to distinguish them from analytical solutions. The L^2-error for μ_* is measured on the arc, while for potentials it is measured on the bounded plane domain Ω, except the arc. The relative error is calculated excluding nodes on which the exact values of test functions are less than h, where h is the step size of the partition. In the numerical result tables for $\tilde{\mu}_*(x)$, M denotes the number of discretized steps on the arc.

6.1 Numerical solution $\tilde{\boldsymbol{\mu}}_*$ of the integral equation

In Sect. 4 we proposed a method for finding the numerical solution of the uniquely solvable integral equation (16). More precisely, we discretized the integral equation and reduced it to the linear algebraic system (26). The solution of the system can be obtained by an inversion of its matrix. Moreover, the solution of the system (26) produces an approximate numerical solution of the original integral equation (16). Now we test this numerical method for solving the integral equation (16) by comparing the numerical solutions with the explicit analytical solutions given by formulas (40)–(42) for certain functions $f(\theta)$ in the right-hand side of the integral equation under the assumption that Γ is an arc of the unit circle. In the tests we have that $\Gamma = \{(r,\theta) \mid r = 1,\ -\pi/3 \le \theta \le \pi/3\}$ is the arc of the unit circle, and $f = 1$ or $f = A\cos(\theta) + B\sin(\theta)$, where $A = B = 1$. Results of the tests are presented in Tables 1 and 2, where the numerical solution $\tilde{\mu}_*$ is compared with the analytical solution μ_*. From these results we obtain numerically that the order of convergence is 3/2 (i.e., convergence is $O(h^{3/2})$) in the L^2-sense for the case of an arc on the unit circle, regardless of the f-type. These results show that the numerical method proposed in Sect. 4 for solving the integral equation (16) by means of solving the linear algebraic system (26) is stable and efficient. In the case of an intercept on a straight line, we obtain excellent numerical results for $\tilde{\mu}_*$, which almost coincide with the analytical solution μ_*, since the integral is equal to zero in the integral equation for this case.

Table 1 An arc on the unit circle: $\beta = 1$, $f = 1$, and $-\pi/3 < \theta < \pi/3$

	$\|\mu_* - \tilde{\mu}_*\|_{L^2(\Gamma)}$		$\|\mu_* - \tilde{\mu}_*\|/\|\mu_*\|$	
M	error	order	error	order
20	$1{\cdot}00266 \times 10^{-3}$		$1{\cdot}09507 \times 10^{-3}$	
40	$3{\cdot}65679 \times 10^{-4}$	1·455	$3{\cdot}98729 \times 10^{-4}$	1·457
80	$1{\cdot}31818 \times 10^{-4}$	1·472	$1{\cdot}43660 \times 10^{-4}$	1·472
160	$4{\cdot}71964 \times 10^{-5}$	1·481	$5{\cdot}14289 \times 10^{-5}$	1·482
320	$1{\cdot}68278 \times 10^{-5}$	1·487	$1{\cdot}83360 \times 10^{-5}$	1·487

Table 2 An arc on the unit circle: $\beta = 1$, $f(\theta) = \cos(\theta) + \sin(\theta)$, and $-\pi/3 < \theta < \pi/3$

	$\|\mu_* - \tilde{\mu}_*\|_{L^2(\Gamma)}$		$\|\mu_* - \tilde{\mu}_*\|/\|\mu_*\|$	
M	error	order	error	order
20	$2{\cdot}48320 \times 10^{-3}$		$2{\cdot}46390 \times 10^{-3}$	
40	$8{\cdot}79158 \times 10^{-4}$	1·498	$8{\cdot}72600 \times 10^{-4}$	1·497
80	$3{\cdot}11218 \times 10^{-4}$	1·498	$3{\cdot}08946 \times 10^{-4}$	1·497
160	$1{\cdot}10141 \times 10^{-4}$	1·498	$1{\cdot}09346 \times 10^{-4}$	1·498
320	$3{\cdot}89701 \times 10^{-5}$	1·498	$3{\cdot}86896 \times 10^{-5}$	1·498

The order of convergence in Tables 1 and 2 has been estimated numerically. Consider the error estimate of the solution μ_* of the integral equation

$$\|\mu_* - \tilde{\mu}_*\| \leq Ch^\gamma \|\mu_*\|, \tag{55}$$

where μ_* is the exact solution and $\tilde{\mu}_*$ is the numerical solution. The constant γ in (55) is the convergence order. Let $\tilde{\mu}_{*,\mathrm{pre}}$ be the numerical solution for the previous step size $(2h)$ satisfying the error estimate

$$\|\mu_* - \tilde{\mu}_{*,\mathrm{pre}}\| \leq C(2h)^\gamma \|\mu_*\|. \tag{56}$$

Hence, by (55) and (56), the convergence order γ can be approximately calculated numerically by the formula

$$\gamma \approx \log_2 \left(\frac{\|\mu_* - \tilde{\mu}_{*,\mathrm{pre}}\|}{\|\mu_* - \tilde{\mu}_*\|} \right).$$

Clearly, if step size h decreases, then the order of convergence converges to γ if the error estimate is correct. We can see this aspect in Tables 1 and 2.

6.2 Tests of computational schemes for potentials

In the recovery of the potentials, $w[\mu](x)$, $v[\mu](x)$, the stiff parts are the integration (5), (10) with logarithmic and angular kernels, since $\mu(s)$ has square-root singularities at the ends of the arc. Because of the singularity of $\mu(s)$ at the ends of the arc, the closer x is to the end of the arc, the less accurate the numerical value of the potential will be. Assume that we calculate the logarithmic potential in the simplest way by replacing it by a summation with a discretized integrand. If x approaches the arc, this summation tends to infinity, since the logarithmic kernel tends to infinity logarithmically at the part of the arc nearest to x. However, it is known that the logarithmic potential is continuous if x moves across the arc. Therefore, the simplest quadrature formula does not preserve the property of continuity of the logarithmic potential when x passes through the arc. Consequently, the numerical value of the single-layer potential calculated by the simplest quadrature formula becomes less accurate at the part of the arc nearest to x. In view of these observations, we modify the formula (10) to (28), (29), so that we select the singular part of the integrand and evaluate the integral with this singular part explicitly. We call this scheme "selection of singularity" as mentioned in Sect. 5.

In computing the angular potential, we calculate the angular kernel as a fixed continuous branch. Besides, we explicitly evaluate the integrals containing the singular parts of μ at the ends of the arc. We call this scheme "direct computation" of the angular potential. This scheme is described in Sect. 5. However, this computational scheme for the angular potential can be improved. Indeed, one can observe that the closer x is to the arc, the steeper the change of the numerical value of the angular kernel on the part of the arc nearest to x will be. Therefore, the accuracy of the angular kernel in the "direct computation" scheme decreases at the parts of the arc nearest to x if x approach the arc. To improve the accuracy of the "direct computation" scheme, we developed a remedial scheme for the angular potential called "subdivision scheme". This scheme decreases the change of angular kernel at the intervals of the arc nearest to x by deviding these intervals into subintervals. The change of the angular kernel at each subinterval is less than on the whole interval; therefore the accuracy of calculating the angular kernel at each subinterval is better than on the whole interval. Hence, after discretization, we can apply the subdivision scheme for recovering the angular potential $v[\mu](x)$ as a remedial scheme.

If the arc Γ is an intercept of a straight line

$$\Gamma = \{x = (x_1, x_2) \,|\, x_2 = 0,\ x_1 = s,\ -1 \leq s \leq 1\}$$

and $\mu(s)$ is given by formula (43), the integrals in the potentials have been evaluated explicitly in formulas (44) and (45) in Sect. 5. We use these explicit expressions for the potentials on the intercept in order

to test our computational schemes developed for potentials and described above. Results of the tests are presented in Tables 3 and 4, where we compare values of the potentials provided by computational schemes (these values are marked by a tilde) and values of potentials provided by their explicit expressions (44) and (45).

Table 3 contains the results of the selection of singularity scheme for the potential $w[\mu]$ and subdivision scheme with 5 sub-steps for potential $v[\mu]$. Table 4 contains the results of a direct computation and subdivision scheme with 5 sub-steps for potential $v[\mu]$ only. As shown in Table 3, the computational schemes described above are stable and efficient for recovering the potentials. The singularity-selection scheme for the single-layer potential produces excellent results and preserves the property of continuity of this potential, when the evaluation point approaches the arc. According to Table 4, the subdivision scheme with 5 sub-steps leads to an improvement for the angular potential in comparison with the direct-computation scheme. This means that the subdivision scheme for the angular potential is more efficient than the direct-computation scheme.

The straight-line case is one of the special cases for problem 2.1. The results for the straight-line case are not sufficient to show that the schemes for recovering the potentials are appropriate for arbitrary arcs. So, we carried out further numerical test for potentials on a curved arc, which is an arc of the unit circle, more precisely, $r = 1$, and $-\pi/3 < \theta < \pi/3$ on the arc. We considered potentials with certain densities having square-root singularities, so that these potentials were evaluated analytically in (53), and (54). We compared the values of the potentials calculated by formulas (53), (54), and values of potentials calculated according to computational schemes described above. In doing so, we used a selection of singularity for the single-layer potential and subdivisions with 5 substeps for the angular potential. The results of this test for the potentials are presented in Table 5. We observe excellent agreement between

Table 3 A straight-line case: $\beta = 1$ with selection of singularity for $w[\mu]$ and subdivision scheme with 5 sub-steps for $v[\mu]$

	$w[\mu]$		$v[\mu]$	
d	$\|w[\mu] - \tilde{w}[\tilde{\mu}]\|_{L^2(\Omega)}$	$\frac{\|w[\mu] - \tilde{w}[\tilde{\mu}]\|}{\|w[\mu]\|}$	$\|v[\mu] - \tilde{v}[\tilde{\mu}]\|_{L^2(\Omega)}$	$\frac{\|v[\mu] - \tilde{v}[\tilde{\mu}]\|}{\|v[\mu]\|}$
	Potentials with number of nodes $M = 160$, $h = 0{\cdot}0125$			
10^{-1}	$1{\cdot}49635 \times 10^{-4}$	$4{\cdot}25109 \times 10^{-4}$	$5{\cdot}51095 \times 10^{-5}$	$5{\cdot}68489 \times 10^{-4}$
10^{-2}	$1{\cdot}75456 \times 10^{-4}$	$5{\cdot}53153 \times 10^{-4}$	$1{\cdot}14253 \times 10^{-4}$	$7{\cdot}16054 \times 10^{-3}$
10^{-3}	$1{\cdot}79021 \times 10^{-4}$	$5{\cdot}87787 \times 10^{-4}$	$7{\cdot}83279 \times 10^{-5}$	$5{\cdot}42667 \times 10^{-3}$
10^{-4}	$1{\cdot}79114 \times 10^{-4}$	$5{\cdot}84952 \times 10^{-4}$	$7{\cdot}72209 \times 10^{-5}$	$5{\cdot}19144 \times 10^{-3}$
10^{-5}	$1{\cdot}79115 \times 10^{-4}$	$5{\cdot}84501 \times 10^{-4}$	$7{\cdot}93442 \times 10^{-5}$	$5{\cdot}36042 \times 10^{-3}$

d = distance from the arc (In this case, arc=$(-1, 1)$: straight line)

Table 4 A straight-line case: $\beta = 1$ with subdivision scheme with 5 sub-steps or direct computing for $v[\mu]$

	Subdivision scheme		Direct computation	
d	$\|v[\mu] - \tilde{v}[\tilde{\mu}]\|_{L^2(\Omega)}$	$\frac{\|v[\mu] - \tilde{v}[\tilde{\mu}]\|}{\|v[\mu]\|}$	$\|v[\mu] - \tilde{v}[\tilde{\mu}]\|_{L^2(\Omega)}$	$\frac{\|v[\mu] - \tilde{v}[\tilde{\mu}]\|}{\|v[\mu]\|}$
	$v[\mu]$ with $M = 160$, $h = 0{\cdot}0125$			
10^{-1}	$5{\cdot}51095 \times 10^{-5}$	$5{\cdot}68489 \times 10^{-4}$	$6{\cdot}12807 \times 10^{-4}$	$6{\cdot}19696 \times 10^{-3}$
10^{-2}	$1{\cdot}14253 \times 10^{-4}$	$7{\cdot}16054 \times 10^{-3}$	$1{\cdot}39909 \times 10^{-3}$	$8{\cdot}72985 \times 10^{-2}$
10^{-3}	$7{\cdot}83279 \times 10^{-5}$	$5{\cdot}42667 \times 10^{-3}$	$3{\cdot}24909 \times 10^{-3}$	$2{\cdot}57348 \times 10^{-1}$
10^{-4}	$7{\cdot}72209 \times 10^{-5}$	$5{\cdot}19144 \times 10^{-3}$	$3{\cdot}68619 \times 10^{-3}$	$2{\cdot}91477 \times 10^{-1}$
10^{-5}	$7{\cdot}93442 \times 10^{-5}$	$5{\cdot}36042 \times 10^{-3}$	$3{\cdot}73361 \times 10^{-3}$	$2{\cdot}95075 \times 10^{-1}$

d = distance from the arc (In this case, arc=$(-1, 1)$: straight line)

Table 5 Arc of the unite circle. Test for the schemes for potentials with selection of singularity for $w[\mu]$ and subdivision scheme with 5 sub-steps for $v[\mu]$

	$\lvert w[\mu_1] - v[\mu_2] - \cos(\pi/3)/2 + x_1/2\rvert$		$\lvert w[\mu_2] + v[\mu_1] + x_2/2\rvert$	
d	L^2-error	Relative error	L^2-error	Relative error
	Number of nodes $M = 160$, $h = \pi/240$			
10^{-1}	$1{\cdot}70043 \times 10^{-4}$	$3{\cdot}33000 \times 10^{-3}$	$1{\cdot}09269 \times 10^{-4}$	$7{\cdot}83636 \times 10^{-3}$
10^{-2}	$2{\cdot}39163 \times 10^{-4}$	$1{\cdot}94430 \times 10^{-2}$	$1{\cdot}29831 \times 10^{-4}$	$5{\cdot}23869 \times 10^{-3}$
10^{-3}	$2{\cdot}38610 \times 10^{-4}$	$1{\cdot}52520 \times 10^{-2}$	$1{\cdot}23720 \times 10^{-4}$	$8{\cdot}50699 \times 10^{-3}$
10^{-4}	$2{\cdot}38548 \times 10^{-4}$	$1{\cdot}46541 \times 10^{-2}$	$1{\cdot}23244 \times 10^{-4}$	$9{\cdot}17430 \times 10^{-3}$
10^{-5}	$2{\cdot}38892 \times 10^{-4}$	$1{\cdot}47696 \times 10^{-2}$	$1{\cdot}23463 \times 10^{-4}$	$9{\cdot}42456 \times 10^{-3}$

d = distance from the arc (In this case, arc=$e^{i\theta}$, $-\pi/3 < \theta < \pi/3$)

the values of the potentials obtained by explicit analytical expressions and values of potentials computed according to our numerical schemes. Finally, summarizing the results shown in Tables 3–5 for the selection-of-singularity scheme for the single-layer potential and for the subdivision scheme with 5 substeps for the angular potential, we can conclude that the uniform relative error of these numerical schemes for the potentials is less than 2 percent if the distance from the arc is more than h, where h is the uniform discretization step of the arc in the computations. In calculating the relative error we drop points, where the absolute value of the exact solution is less than h. Moreover, if the distance from the arc is less than h, the uniform relative error in our method is less than 2 percent, as well.

7 Simulation of electric properties in semiconductor film

This section contains results of a simulation of the electric properties in a semiconductor film. To obtain these results we solved problem 2.1 numerically as described above. First, we found the approximate numerical solution $\mu(s)$ of the integral equation (16) by solving numerically the linear algebraic system (26). Next we substituted $\mu(s)$ in the solution of problem 2.1 given by formula (9) and computed the potentials according to the schemes described above. Below, for all simulations presented in the figures, we use a selection-of-singularity scheme for the single-layer potential and a subdivision scheme with 5 substeps for the angular potential. Thus, we obtain the numerical solution $u[\mu]$ of problem 2.1. Recall that $u[\mu]$ is the electric potential. Electric intensity and electric current can be found using formulas from Sect. 2.

Results of simulation are given in the figures. The figures present the electric current on the left, field potential and intensity on the right.

7.1 Simulation if the arc is an intercept of a straight line

The Figs. 1–4 show the results of simulations if the arc

$$\Gamma = \{x = (x_1, x_2) \,|\, x_2 = 0,\ x_1 = s,\ -1 \le s \le 1\}$$

is an intercept of the straight line.

The Figs. 1–3 present a simulation with $f = 1$, but for different values of β, while Fig. 4 presents a simulation with $f(s) = \cos(s) + \sin(s)$, where s is the arc length parameter, i.e., $s = x_1$ on the intercept.

We observe in Figs. 2, 3 that, if $\beta \neq 0$, then the symmetric aspect of the electric field is broken. Figs. 1, 3, 4 display the Hall effect, i.e., since $\beta \neq 0$, there is a nonzero angle between the electric-intensity vector and the vector of the electric current. Moreover, this angle increases if $|\beta|$ increases. Clearly, if a magnetic field is absent ($\beta = 0$), then the intensity vector and the current vector have the same direction. An extreme for value of β case is shown in Fig. 1 where $\beta = -10$.

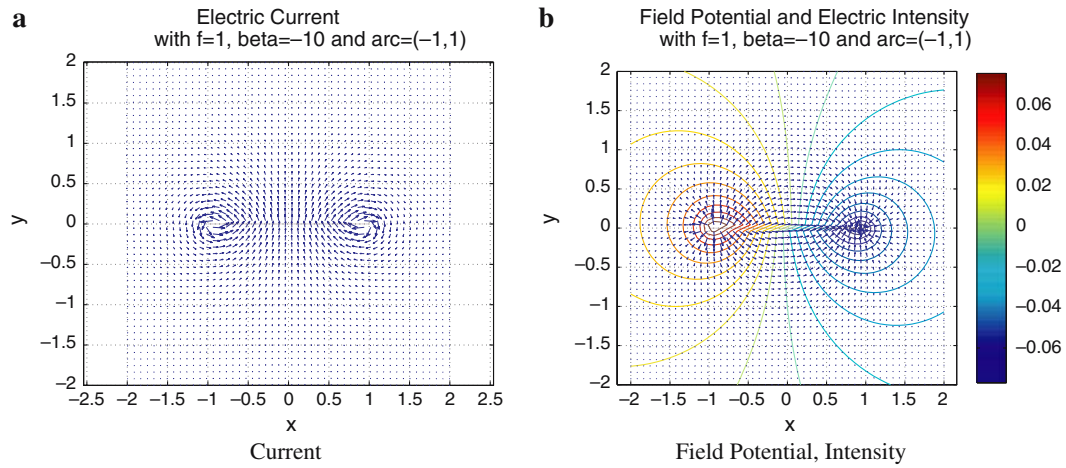

Fig. 1 Straight-line case: current, field potential, and intensity with $\beta = -10, f = 1$, and $s \in (-1, 1)$

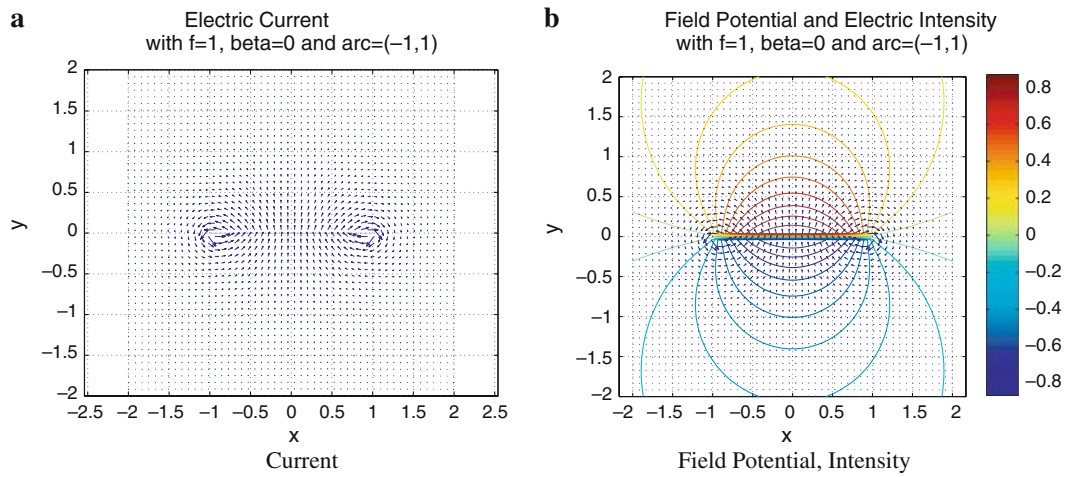

Fig. 2 Straight-line case: current, field potential, and intensity with $\beta = 0, f = 1$, and $s \in (-1, 1)$

The simulated case with $f(s) = \cos(s) + \sin(s)$ has no analytic solution. Hence, we can only expect the physical phenomenon to be obtained from the numerical solution. In Fig. 4, the electric current is stronger around $x_1 = 1$ than around $x_1 = -1$ because of the influence of $f(s) = \cos(s) + \sin(s)$. As to the electric intensity, we can observe that the intensity with $f = 1$ is symmetric with respect to the origin in space, while the intensity with $f(s) = \cos(s) + \sin(s)$ is strengthened at the right upper part on the arc. These observations show a reasonable aspect of the above electric properties of the plane semiconductor film with the constant magnetic field acting in a direction normal to the plane.

If Γ is an intercept of a straight line, the direction of the electric current at each point does not depend on β; it depends on f only. This effect can be observed in Figures 1–3, and it can be explained analytically. Let

$$\mathbf{j} = (j_1, j_2) = \frac{(1+\beta^2)}{\eta}\mathbf{J},$$

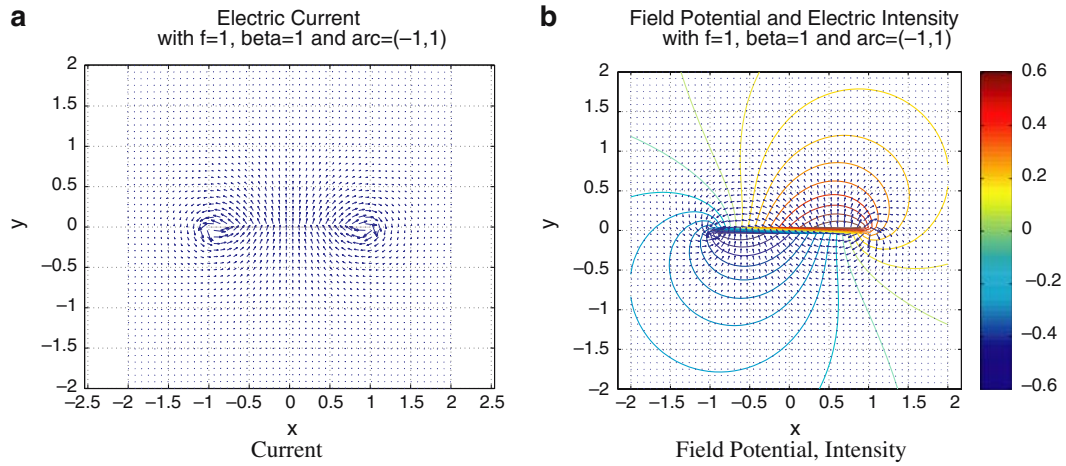

Fig. 3 Straight-line case: current, field potential, and intensity with $\beta = 1, f = 1$, and $s \in (-1, 1)$

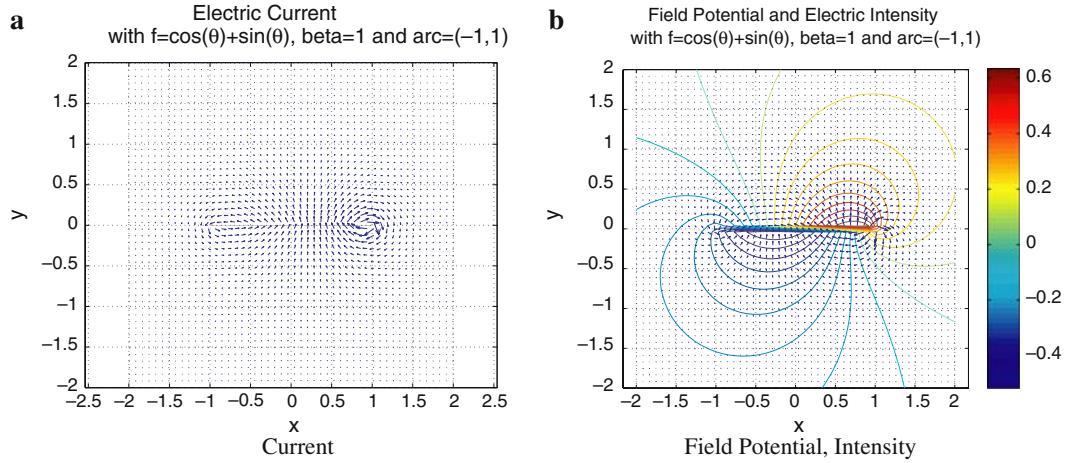

Fig. 4 Straight-line case: current, field potential, and intensity with $\beta = 1, f(s) = \cos(s) + \sin(s)$, and $s \in (-1, 1)$

where $\mathbf{J} = (J_1, J_2)$ is the electric-current density. Therefore, the electric current $\mathbf{J}$ has the same direction as the vector $\mathbf{j}$ at each point. Let the electric potential be $u(x)$. Then

$$\Phi_0(z) = -\left(u_{x_1} - \mathrm{i}u_{x_2}\right)(1 + \mathrm{i}\beta) = j_1 - \mathrm{i}j_2$$

is an analytic complex function for $z = x_1 + \mathrm{i}x_2$. The boundary condition of problem 2.1 can be rewritten in the form $\Im\mathfrak{m}(\Phi_0) = -f$ on the intercept Γ.

Hence, we obtain the following problem: find an analytic complex function $\Phi_0(z)$ outside an intercept so that its imaginary part on the intercept Γ is known and equal to $-f$. The solution of this problem does not depend on β. If we find $\Phi_0(z)$, the vector $\mathbf{j}$ is determined as $\mathbf{j} = (j_1, j_2) = (\Re\mathfrak{e}(\Phi_0), -\Im\mathfrak{m}(\Phi_0))$. This formulation does not depend on β, so our numerical results presented in Figures 1–3 are reasonable since they show that the direction of the electric current is also independent of β.

7.2 Simulation for the arc of the unit circle

Figures 5–8 present simulation results, when Γ is an arc of the unit circle. We found two interesting phenomena if Γ is an arc of the circle. One of them is that the direction of the electric current at each point

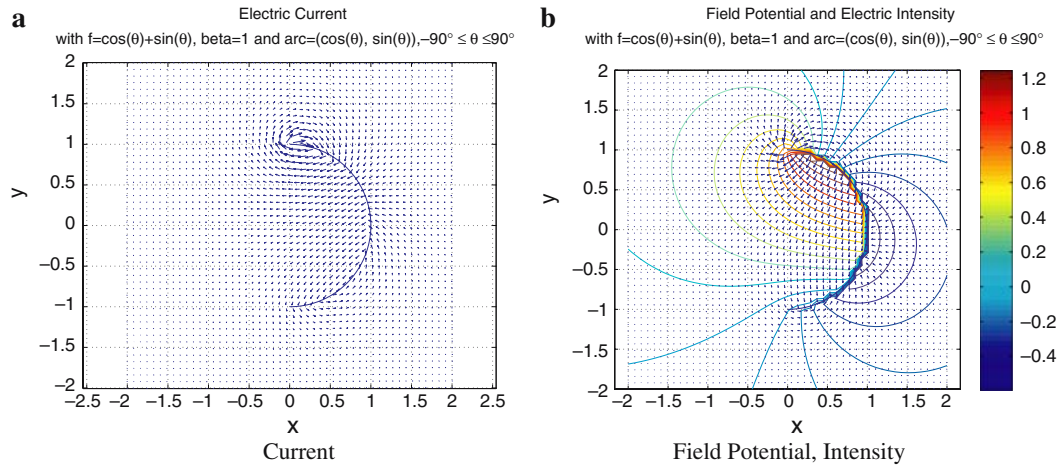

Fig. 5 Open-arc case: current, field potential, and intensity with $\beta = 1, f(\theta) = \cos(\theta) + \sin(\theta)$, and $-90° < \theta < 90°$

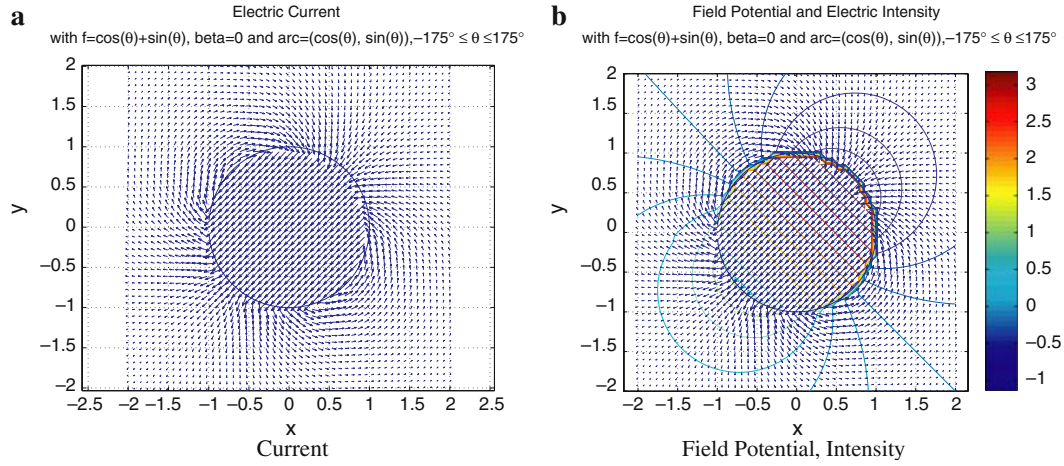

Fig. 6 Open-arc case: current, field potential, and intensity with $\beta = 0, f(\theta) = \cos(\theta) + \sin(\theta)$, and $-175° < \theta < 175°$

does not depend on β; it depends on f only. This phenomenon, shown in Figures 5 and 8, can be explained analytically. Let

$$\mathbf{j} = (j_1, j_2) = \frac{(1+\beta^2)}{\eta}\mathbf{J},$$

where $\mathbf{J} = (J_1, J_2)$ is the electric-current density. Therefore, the electric current $\mathbf{J}$ has the same direction as the vector $\mathbf{j}$ at each point. Let the electric potential be $u(x)$. Then

$$\Phi_1(z) = -z\left(u_{x_1} - \mathrm{i}u_{x_2}\right)(1 + \mathrm{i}\beta) = z\,(j_1 - \mathrm{i}j_2)$$

is an analytic complex function for $z = x_1 + \mathrm{i}x_2$. The boundary condition of problem 2.1 can be rewritten in the form $\mathfrak{Re}(\Phi_1) = -f$ on the arc of the circle.

Hence, we can obtain the following problem: find an analytic complex function $\Phi_1(z)$ outside an arc so that its real part on the arc is known and equal to $-f$. The solution of this problem does not depend on β. If we find $\Phi_1(z)$, the vector $\mathbf{j}$ is determined as $\mathbf{j} = (j_1, j_2) = (\mathfrak{Re}(\Phi_1/z), -\mathfrak{Im}(\Phi_1/z))$. This formulation does not depend on β, so our numerical results are reasonable since they show that the direction of the electric current is also independent of β.

The second phenomenon shown by our results is a very interesting effect, which is called disappearance of singularity. Assume that Γ is an arc of the unit circle, $s = \theta \in [-\pi/2, \pi/2]$, and consider the function

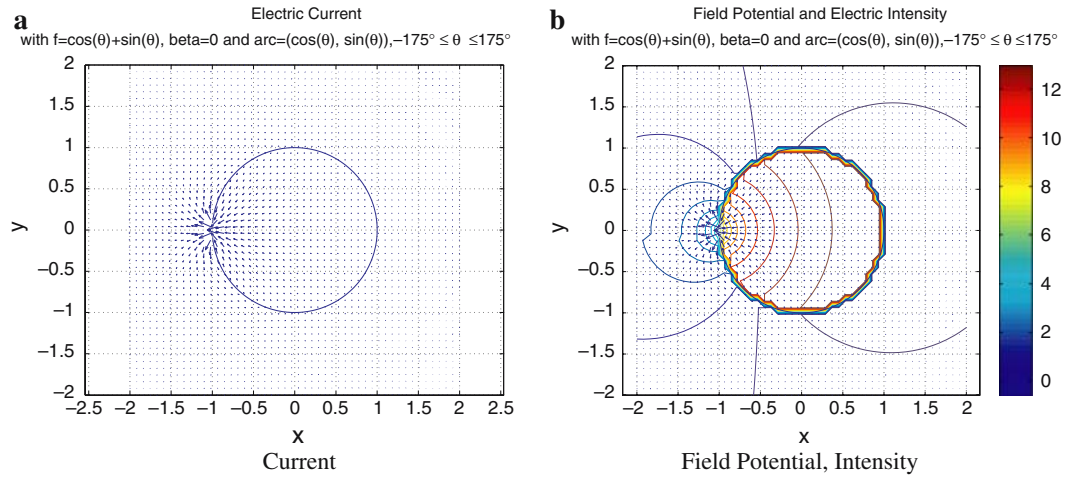

Fig. 7 Open-arc case: current, field potential, and intensity with $\beta = 0, f = 1$, and $-175^\circ < \theta < 175^\circ$

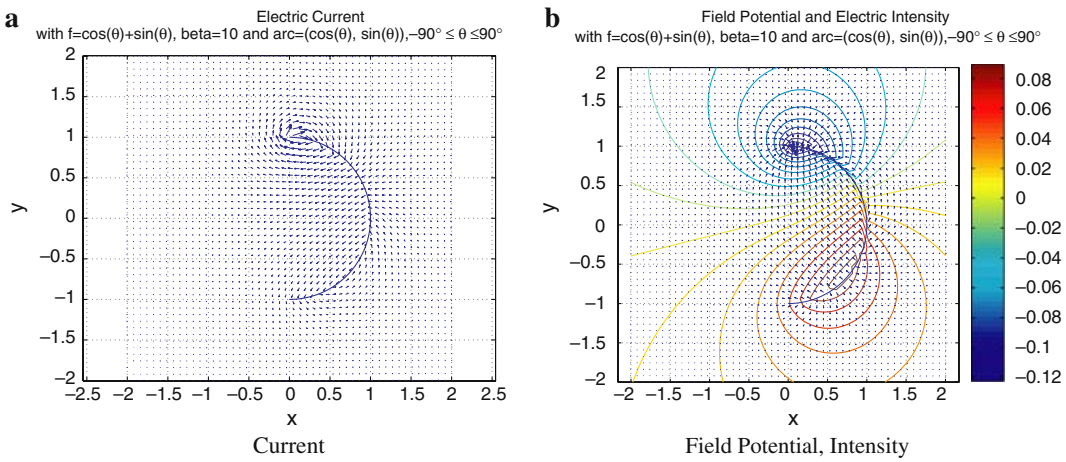

Fig. 8 Open-arc case: current, field potential, and intensity with $\beta = -10, f(\theta) = \cos(\theta) + \sin(\theta)$, and $-90^\circ < \theta < 90^\circ$

$f(s) = \cos s + \sin s$ in (3). Our numerical simulation show (see Figs. 5 and 8) that the intensity of the electric field and the electric current do not have a singularity at the end $s = -\pi/2$ for any β, although the intensity and current have singularities at the end $s = \pi/2$. This is true since $\mu(s)$ does not have a square-root singularity if $s \to -\pi/2$, while it has a square-root singularity if $s \to \pi/2$. Indeed, it follows from (42), with $A = B = 1$, that $\mu(s) \to 0$ if $s \to -\pi/2$, while $\mu(s) \approx \dfrac{\mathcal{C}_0}{\sqrt{\pi/2 - s}}$ if $s \to \pi/2$, where $\mathcal{C}_0 \neq 0$ is a constant. This effect is also independent of β.

Set $x_1 = r\cos\theta,\ x_2 = r\sin\theta$. If Γ is a closed unit circumference, i.e., closed curve, and $f(\theta) = \cos\theta + \sin\theta$, then the solution of problem 2.1 inside the unit circle ($r < 1$) exists and can be written in explicit form:

$$u = \frac{(x_1(A - B\beta) + x_2(B + A\beta))}{(1 + \beta^2)} + C,$$

where C is an arbitrary constant and $A = B = 1$. In this case, the components of the electric current inside the unit circle are

$$J_1 = J_2 = -\frac{\eta}{(1 + \beta^2)}.$$

Now let Γ be an open arc on the unit circumference:

$$\Gamma = \{(x_1, x_2) : \ r = 1, \ \ -175^\circ \le \theta \le 175^\circ\}. \tag{57}$$

Since open arc (57) is close to the closed unit circumference, we can predict that the solution of problem 2.1 with open arc (57) and with $f(\theta) = \cos\theta + \sin\theta$ must be close to the aforementioned explicit solution of problem 2.1 inside the unit circle. The numerical solution of problem 2.1 with open arc (57) and with $f(\theta) = \cos\theta + \sin\theta$ is presented in Fig. 6 for $\beta = 0$. If $r < 1$, we observe excellent agreement between the numerical solution presented in Fig. 6 and the explicit analytical solution written above for a closed circumference Γ.

We can observe a very interesting phenomenon in Fig. 7 by replacing above $f(\theta) = \cos(\theta) + \sin(\theta)$ by $f = 1$. If Γ is a unit circumference (closed curve), our problem with $\beta = 0$ transforms to the Neumann problem, which does not have a solution both inside and outside the whole circle because $f = 1$. Indeed, if Γ is a closed unit circumference, the condition of solvability of our Neumann problem both inside and outside the whole circle does not hold since

$$\int_{-\pi}^{\pi} f(\theta) \mathrm{d}\theta \neq 0.$$

However, the problem for a nonclosed arc $-175^\circ \le \theta \le 175^\circ$ has the solution presented in Fig. 7. In this case the strength of the electric current is relatively strong near the hole between ends of the arc. The inside current flux concentrates at the hole which is between the end points of the arc, and after passing the hole, the current flux is on a steep descent.

8 Conclusions

The problem studied in the present paper has not been treated numerically before. A new computational method for solving this problem has been suggested. Our numerical approach to problem 2.1 consists of two parts. The first part is solving the integral equation (16). The second part is the recovery of single-layer and angular potentials (5), (10) by applying modified computational schemes. For the computation of the single-layer potential we used the selection-of-singularity formulas (28), (29). For the computation of the angular potential we used direct computation (36) or a subdivision scheme. The subdivision scheme is essential for computing the angular potential near the arc, where the angular kernel is rapidly changing, which is similar to a jump phenomenon, when the function is not continuously smooth. The modified schemes allow us to overcome the square-root singularities at the end points of the arc and to overcome the decrease of accuracy for the numerical solutions at the points whose distance from the arc is less than h.

The developed numerical method enables us to compute a numerical solution of problem 2.1 for an arc Γ of arbitrary shape. Moreover, our tests show that the uniform relative error of the numerical schemes for the potentials is less than 2 percent if the distance from the arc is more than h, where h is the uniform discretization step of the arc in the computations. In calculating the relative error we drop points, where the absolute value of the exact solution is less than h. If the distance from the arc is less than h, then the uniform relative error in our method is less than 2 percent as well. This is the advantage of our method in comparison with known numerical methods for Dirichlet and Neumann harmonic problems in the exterior of an arc in a plane.

Tables 2 and 5 show that the basic decrease of accuracy in our computational algorithm takes place in the second part, when we compute the potentials. The accuracy in the first part, when solving the integral equation, is a 100 times better than in the second part. Therefore the accuracy in our approach is limited by the accuracy produced in the second part. It seems that the numerical method for solving the integral equation proposed in this paper is optimal for our problem. There are several modern methods [1, Part IV], [12, Part II], [13], [14, Chapter 11] for solving the singular integral equation. The methods proposed

in [13], [14, Chapter 11] produce very high accuracy if the function f in (3) is sufficiently smooth. However it is not reasonable for us to increase the accuracy when computing the integral equation, since the final accuracy of the numerical solution to problem 2.1 is limited by the accuracy in the second part, when the potentials are computed. The method of discrete vortices proposed in [1, Part IV], [12, Part II] for solving the singular integral equation is very simple, and so it is very popular in the engineering community. However, the accuracy guaranteed by this method is comparable with the accuracy in the second part of our approach, i.e., the accuracy of this method may decrease the total accuracy of the numerical solution of problem 2.1. Nevertheless, all methods proposed in [1, Part IV], [12, Part II], [13], [14, Chapter 11] are applicable to solving the singular integral equation in our problem.

It should be noted that the accuracy obtained for the computation of the potentials near the boundary in the second part of our approach is high enough in comparison with the accuracy produced by standard methods for potentials. This is achieved by using an analytical evaluation of the singular part in the single-layer potential and by using the angular potential instead of a double-layer potential. The singularity of the kernel in the angular potential is less than in the double-layer potential; therefore the angular potential can be calculated near the boundary with better accuracy than the double-layer potential. However, the numerical methods for the computation of the angular potential have not been developed previously, although this potential was already introduced in 1977 in [8]. It seems that the present paper is the first attempt to construct a numerical method for the computation of the angular potential. The kernel of the angular potential is a multi-valued function, and a correct selection of its branch in each computational point produces the principal difficulty of the computational scheme. The algorithm for the computation of the angular kernel is presented in Sect. A.4 of the Appendix.

Appendix, Some derivations

A.1. Detailed derivation of $\frac{1}{\pi}\int_a^b \frac{Q(\sigma)}{\sigma - s}\mathrm{d}\sigma$, equality (18)

Consider the complex function $q(z) = \sqrt{z-a}\sqrt{z-b}$ outside the cut L lying on the real axis: $L = \{z : \Im\mathrm{m}\, z = 0,\ a < \Re\mathrm{e}\, z < b\}$, then $q(t)|_{t\in L^+} = \mathrm{i}Q(s)$, $q(t)|_{t\in L^-} = -\mathrm{i}Q(s)$ $(t = s \text{ on } L)$. The side of the cut L which is situated on the left, when $\Re\mathrm{e}\, z$ increases on L, is denoted by L^+, while the opposite side is denoted by L^-. Let $q(t)|_{t\in L^+} = q(t)$, $q(t)|_{t\in L^-} = -q(t)$, $q(t) = \mathrm{i}Q(t)$. We fix the branches of the analytic complex function $q(z)$ ($q(z)$ is analytic in the exterior of L) so that

$$q(z)|_{\Im\mathrm{m}\, z=0,\ \Re\mathrm{e}\, z>b} > 0, \qquad q(z)|_{\Im\mathrm{m}\, z=0,\ \Re\mathrm{e}\, z<a} < 0.$$

$$\text{Compute } \frac{1}{\pi}\int_a^b \frac{Q(\sigma)}{\sigma - s}\mathrm{d}\sigma = I_0(s) = \frac{1}{\pi\mathrm{i}}\int_a^b \frac{q(t)}{t-s}\mathrm{d}t\,.$$

Consider the following integral of the Cauchy type:

$$\Psi(z) = \frac{1}{2\pi\mathrm{i}}\int_a^b \frac{q(t)}{t-z}\mathrm{d}t;$$

then, according to the Plemelj formulas for integrals of this type [10, Sect. 16], we have on L: $I_0(t_0) = \Psi^+(t_0) + \Psi^-(t_0)$ and $\Psi^+(t_0) - \Psi^-(t_0) = q(t_0)$, where $\Psi^{\pm}(t_0) = \lim\limits_{z\to t_0\in L^{\pm}} \Psi(z)$. Consequently, the function $\Psi(z)$ is a solution of the following jump problem.

Jump problem: To find a piecewise holomorphic function $\Psi(z)$ with the line of jumps L satisfying the boundary condition: $\Psi^+(t_0) - \Psi^-(t_0) = q(t_0)$ on L and such that $\Psi(\infty) = 0$.

One can show [10, Sect. 31] that the solution of the above jump problem is unique. Let $c_0 = \dfrac{a+b}{2}$. It can be verified directly that the function $\left(\dfrac{1}{2}q(z) - \dfrac{z-c_0}{2}\right)$ also satisfies the same jump problem. In particular, this function tends to 0 as $z \to \infty$ in view of the following relationships:

$$\sqrt{z-a} = \sqrt{z}\sqrt{1-\frac{a}{z}} = \sqrt{z}\left(1 - \frac{a}{2z} + o\left(\frac{1}{z}\right)\right),$$

$$q(z) = z\ \left(1 - \frac{a+b}{2z} + o\left(\frac{1}{z}\right)\right) = z - \frac{a+b}{2} + o(1) = z - c_0 + o(1).$$

According to the uniqueness of the solution of the jump problem, we have $\Psi(z) = \dfrac{1}{2}q(z) - \dfrac{z-c_0}{2}$. Therefore

$$I_0(s) = \Psi^+(s) + \Psi^-(s) = (c_0 - s) = \frac{a+b}{2} - s;$$

finally

$$I_0(s) = \frac{1}{\pi}\int_a^b \frac{Q(\sigma)}{\sigma - s}\mathrm{d}\sigma = \frac{a+b}{2} - s.$$

A.2. Detailed derivation of selection of singularity

Here the integrals I and J from (30), (31) will be calculated. Let us start from the integral

$$I = \int\limits_{s_j-h/2}^{s_j+h/2} \frac{\log[(\sigma - s_j - c)^2 + d^2]}{\sqrt{\sigma - a}}\mathrm{d}\sigma, \qquad s_j - h/2 \geq a.$$

Set $\sigma = s_j + \upsilon$, $s_j - a = \phi$; then

$$I = \int\limits_{-h/2}^{h/2} \frac{1}{\sqrt{\upsilon + \phi}} \log[(\upsilon - c)^2 + d^2]\mathrm{d}\upsilon.$$

First, we consider the case $d \neq 0$. After integration by parts, we obtain:

$$I = 2\sqrt{\phi + \frac{h}{2}}\ \log\left[\left(c - \frac{h}{2}\right)^2 + d^2\right] - 2\sqrt{\phi - \frac{h}{2}}\ \log\left[\left(c + \frac{h}{2}\right)^2 + d^2\right] - 4I_1,$$

where

$$I_1 = \int\limits_{-h/2}^{h/2} \frac{\sqrt{\upsilon + \phi}\,(\upsilon - c)}{(\upsilon - c)^2 + d^2}\mathrm{d}\upsilon.$$

Let us denote: $\sqrt{\upsilon + \phi} = \xi$, $\phi + c = g$; then

$$I_1 = 2\int\limits_{\sqrt{\phi-h/2}}^{\sqrt{\phi+h/2}} \frac{\xi^2(\xi^2 - g)}{(\xi^2 - g)^2 + d^2}\mathrm{d}\xi = 2\left(I_3\left(\sqrt{\phi + h/2}\right) - I_3\left(\sqrt{\phi - h/2}\right)\right),$$

where

$$I_3(\xi) = \int \frac{\xi^2(\xi^2 - g)}{(\xi^2 - g)^2 + d^2}\mathrm{d}\xi.$$

Hence, if we know $I_3(\xi)$, we can finally get I:

$$I = 2\sqrt{\phi + \tfrac{h}{2}}\,\log\left[\left(c - \tfrac{h}{2}\right)^2 + d^2\right] - 2\sqrt{\phi - \tfrac{h}{2}}\,\log\left[\left(c + \tfrac{h}{2}\right)^2 + d^2\right] -$$

$$-8I_3\left(\sqrt{\phi + \frac{h}{2}}\right) + 8I_3\left(\sqrt{\phi - \frac{h}{2}}\right).$$

The following integral

$$J = \int_{s_j - h/2}^{s_j + h/2} \frac{\log[(\sigma - s_j - c)^2 + d^2]}{\sqrt{b - \sigma}}\mathrm{d}\sigma, \qquad s_j + h/2 \le b$$

in the case $d \neq 0$ can be calculated similarly:

$$J = 2\sqrt{\kappa + \tfrac{h}{2}}\,\log\left[\left(c + \tfrac{h}{2}\right)^2 + d^2\right] - 2\sqrt{\kappa - \tfrac{h}{2}}\,\log\left[\left(c - \tfrac{h}{2}\right)^2 + d^2\right] +$$

$$+8J_3\left(\sqrt{\kappa - \frac{h}{2}}\right) - 8J_3\left(\sqrt{\kappa + \frac{h}{2}}\right),$$

where

$$J_3(\zeta) = \int \frac{\zeta^2(\zeta^2 - l)}{(\zeta^2 - l)^2 + d^2}\mathrm{d}\zeta,$$

and $\kappa = b - s_j,\ l = \kappa - c$.

In the calculation, $J_3(\zeta)$ is similar to $I_3(\xi)$. Now we will calculate $I_3(\xi)$. First, from the integrand of $I_3(\xi)$, we obtain

$$\frac{\xi^2(\xi^2 - g)}{(\xi^2 - g)^2 + d^2} = 1 + \frac{g\xi^2 - g^2 - d^2}{(\xi^2 - g)^2 + d^2},$$

whence

$$I_3(\xi) = \xi + I_4(\xi), \text{ with } I_4(\xi) = \int \frac{g\xi^2 - g^2 - d^2}{(\xi^2 - g)^2 + d^2}\mathrm{d}\xi.$$

The integrand of $I_4(\xi)$ is written as below:

$$\frac{g\xi^2 - g^2 - d^2}{(\xi^2 - g)^2 + d^2} = \frac{\mathcal{A}\xi + \mathcal{B}}{\xi^2 + p\xi + q} - \frac{\mathcal{A}\xi - \mathcal{B}}{\xi^2 - p\xi + q},$$

where $q = \sqrt{g^2 + d^2}$, $p = \sqrt{2(q + g)}$, $\mathcal{A} = -\dfrac{p}{4}$, $\mathcal{B} = -\dfrac{q}{2}$. We can now divide $I_4(\xi)$ into two integrals $I_5(\xi)$, and $I_6(\xi)$,

$$I_4(\xi) = I_5(\xi) - I_6(\xi),$$

where

$$I_5(\xi) = \int \frac{\mathcal{A}\xi + \mathcal{B}}{\xi^2 + p\xi + q}\mathrm{d}\xi, \quad I_6(\xi) = \int \frac{\mathcal{A}\xi - \mathcal{B}}{\xi^2 - p\xi + q}\mathrm{d}\xi.$$

Now, $I_5(\xi)$ is calculated easily

$$I_5(\xi) = \frac{\mathcal{A}}{2}\log(\xi^2 + p\xi + q) - m\arctan\frac{2\xi + p}{4m},$$

with

$$m = \frac{1}{2}\sqrt{\frac{q-g}{2}}.$$

We omit the additive constants, because they cancel in the final expression. And also $I_6(\xi)$ is calculated

$$I_6(\xi) = \frac{\mathcal{A}}{2}\log(\xi^2 - p\xi + q) + m\arctan\frac{2\xi - p}{4m}.$$

We obtain:

$$I_4(\xi) = \frac{\mathcal{A}}{2}\log\frac{\xi^2 + p\xi + q}{\xi^2 - p\xi + q} - m\left(\arctan\frac{2\xi + p}{4m} + \arctan\frac{2\xi - p}{4m}\right),$$

$$I_3(\xi) = \xi + \frac{p}{8}\log\frac{\xi^2 - p\xi + q}{\xi^2 + p\xi + q} - m\left(\arctan\frac{2\xi + p}{4m} + \arctan\frac{2\xi - p}{4m}\right).$$

Similarly, we get

$$J_3(\zeta) = \zeta + \frac{\tilde{p}}{8}\log\frac{\zeta^2 - \tilde{p}\zeta + \tilde{q}}{\zeta^2 + \tilde{p}\zeta + \tilde{q}} - \tilde{m}\left(\arctan\frac{2\zeta + \tilde{p}}{4\tilde{m}} + \arctan\frac{2\zeta - \tilde{p}}{4\tilde{m}}\right),$$

where $\tilde{q} = \sqrt{l^2 + d^2}, \tilde{p} = \sqrt{2(\tilde{q} + l)}, \tilde{m} = \frac{1}{2}\sqrt{\frac{\tilde{q} - l}{2}}$. This completes the derivation of I and J for the case of $d \neq 0$.

For the other case, $d = 0$, we obtain

$$I = 2\sqrt{\phi + \frac{h}{2}}\,\log\left[\left(c - \frac{h}{2}\right)^2\right] - 2\sqrt{\phi - \frac{h}{2}}\,\log\left[\left(c + \frac{h}{2}\right)^2\right] - 4I_1,$$

where $c \neq \frac{h}{2}, c \neq -\frac{h}{2}$, and

$$I_1 = \int_{-h/2}^{h/2} \frac{\sqrt{\upsilon + \phi}}{(\upsilon - c)}\mathrm{d}\upsilon.$$

Let us denote: $\sqrt{\upsilon + \phi} = \xi, \quad \phi + c = g$; then

$$I_1 = 2\int_{\sqrt{\phi - h/2}}^{\sqrt{\phi + h/2}} \frac{\xi^2}{(\xi^2 - g)}\mathrm{d}\xi = 2\left(I_3\left(\sqrt{\phi + h/2}\right) - I_3\left(\sqrt{\phi - h/2}\right)\right),$$

where

$$I_3(\xi) = \int \frac{\xi^2}{(\xi^2 - g)}\mathrm{d}\xi.$$

Now we calculate $I_3(\xi)$,

$$I_3(\xi) = \xi + \int \frac{g}{\xi^2 - g}\mathrm{d}\xi$$

(i) $g \geq 0$,

$$\begin{aligned}\int \frac{g}{\xi^2 - g}\mathrm{d}\xi &= \frac{1}{2}\left(\int \frac{\sqrt{g}}{\xi - \sqrt{g}}\mathrm{d}\xi - \int \frac{\sqrt{g}}{\xi + \sqrt{g}}\mathrm{d}\xi\right)\\ &= \frac{1}{2}\sqrt{g}\left(\log\left|\xi - \sqrt{g}\right| - \log\left|\xi + \sqrt{g}\right|\right)\\ &= \frac{1}{2}\sqrt{g}\,\log\left|\frac{\xi - \sqrt{g}}{\xi + \sqrt{g}}\right|\end{aligned}$$

(ii) $g < 0$,

$$\int \frac{g}{\xi^2 - g}\mathrm{d}\xi = \int \frac{g}{\xi^2 + (\sqrt{-g})^2}\mathrm{d}\xi$$
$$= g\int \frac{1}{\xi^2 + (\sqrt{-g})^2}\mathrm{d}\xi = -\sqrt{-g}\arctan\left(\frac{\xi}{\sqrt{-g}}\right)$$

Hence,

$$I_3(\xi) = \begin{cases} \xi + \frac{1}{2}\sqrt{g}\log\left|\frac{\xi-\sqrt{g}}{\xi+\sqrt{g}}\right| & \text{if } g \geq 0 \\ \xi - \sqrt{-g}\arctan\left(\frac{\xi}{\sqrt{-g}}\right) & \text{if } g < 0 \end{cases} \tag{58}$$

Using this expression for $I_3(\xi)$ we get I for $d = 0$ as follows:

$$I = 2\sqrt{\phi + \frac{h}{2}}\log\left[\left(c - \frac{h}{2}\right)^2\right] - 2\sqrt{\phi - \frac{h}{2}}\log\left[\left(c + \frac{h}{2}\right)^2\right]$$
$$-8\left(I_3\left(\sqrt{\phi + \frac{h}{2}}\right) - I_3\left(\sqrt{\phi - \frac{h}{2}}\right)\right)$$

where $c \neq \frac{h}{2}$ and $c \neq -\frac{h}{2}$.

Similarly, we can calculate J in case of $d = 0$. If $d = 0$,

$$J = 2\sqrt{\kappa + \tfrac{h}{2}}\log\left[\left(c + \tfrac{h}{2}\right)^2\right] - 2\sqrt{\kappa - \tfrac{h}{2}}\log\left[\left(c - \tfrac{h}{2}\right)^2\right]$$
$$+8J_3\left(\sqrt{\kappa - \frac{h}{2}}\right) - 8J_3\left(\sqrt{\kappa + \frac{h}{2}}\right),$$

where $c \neq \frac{h}{2}$, $c \neq -\frac{h}{2}$, and

$$J_3(\zeta) = \int \frac{\zeta^2}{(\zeta^2 - l)}\mathrm{d}\zeta, \qquad \text{with} \quad l = \kappa - c, \quad \kappa = b - s_j.$$

Hence, $J_3(\zeta)$ is similar to $I_3(\xi)$ for $d = 0$. The function $J_3(\zeta)$ is given by formula (58), where we must replace ξ by ζ and g by l. We complete the derivation of the integrals I and J for the basic cases.

Note that the logarithmic potential is continuous when point x passes across the arc of integration. However, the simplest quadrature formula for the logarithmic potential produces a logarithmic singularity, when x approaches the arc, because of the logarithmic singularity in the integrand of the potential. This logarithmic singularity is integrated in the formulas for I and J, as well as the square-root singularity at the ends of the arc. The integrals I and J produce an advanced formula for the numerical computation of the logarithmic potential. This advanced formula does not have any singularity if the point x (contained in the parameters c and d in I and J) approaches the arc. In other words, this advanced formula for numerical computation preserves the property of continuity across the arc for the logarithmic potential, unlike the simplest quadrature formulas.

A.3. Detailed derivation of equalities (39), (41), (42)

Let Γ be an arc of a unit circumference: $x = (\cos\theta_0, \sin\theta_0) \in \Gamma$ for $\theta_0 \in [a, b]$, $\mathbf{n} = (\cos\theta_0, \sin\theta_0)$, $\boldsymbol{\tau} = (-\sin\theta_0, \cos\theta_0)$, and a, b are polar angles of endpoints such that $-\pi < a < b < \pi$. Then

$$|x - y| = |\mathrm{e}^{\mathrm{i}\theta_0} - \mathrm{e}^{\mathrm{i}\theta}| = 2\left|\sin\frac{\theta_0 - \theta}{2}\right|, \quad \forall y = (\cos\theta, \sin\theta) \in \Gamma, \tag{59}$$

and

$$\frac{x_1 - y_1}{|x-y|} = \frac{\cos\theta_0 - \cos\theta}{|x-y|} = -\mathrm{sgn}[\theta_0 - \theta]\sin\frac{\theta_0+\theta}{2},$$

$$\frac{x_2 - y_2}{|x-y|} = \frac{\sin\theta_0 - \sin\theta}{|x-y|} = \mathrm{sgn}[\theta_0 - \theta]\cos\frac{\theta_0+\theta}{2},$$

where

$$\cos\theta_0 - \cos\theta = \mathfrak{Re}\left(\mathrm{e}^{\mathrm{i}\theta_0} - \mathrm{e}^{\mathrm{i}\theta}\right) = \mathfrak{Re}\left(\mathrm{e}^{\mathrm{i}\frac{\theta_0+\theta}{2}}\left(2\mathrm{i}\sin\frac{\theta_0-\theta}{2}\right)\right)$$
$$= -2\sin\frac{\theta_0+\theta}{2}\sin\frac{\theta_0-\theta}{2},$$

$$\sin\theta_0 - \sin\theta = \mathfrak{Im}(\mathrm{e}^{\mathrm{i}\theta_0} - \mathrm{e}^{\mathrm{i}\theta}) = \mathfrak{Im}\left(\mathrm{e}^{\mathrm{i}\frac{\theta_0+\theta}{2}}\left(2\mathrm{i}\sin\frac{\theta_0-\theta}{2}\right)\right)$$
$$= 2\cos\frac{\theta_0+\theta}{2}\sin\frac{\theta_0-\theta}{2},$$

and

$$\mathrm{sgn}\left[\sin\frac{\theta_0-\theta}{2}\right] = \mathrm{sgn}\left[\frac{\theta_0-\theta}{2}\right] = \mathrm{sgn}\left[\theta_0-\theta\right],$$

since $-\pi < a < b < \pi$. According to (17)

$$\sin\varphi_0(x,y) = -\frac{x_1-y_1}{|x-y|}\cos\alpha - \frac{x_2-y_2}{|x-y|}\sin\alpha$$
$$= -\mathrm{sgn}[\theta_0-\theta]\sin\frac{\theta_0+\theta}{2}\sin\theta_0 - \mathrm{sgn}[\theta_0-\theta]\cos\frac{\theta_0+\theta}{2}\cos\theta_0$$
$$= -\mathrm{sgn}[\theta_0-\theta]\cos\frac{\theta-\theta_0}{2},$$

since $\boldsymbol{\tau} = (\cos\alpha, \sin\alpha) = (-\sin\theta_0, \cos\theta_0)$. Using (59) and other above relationships we obtain

$$\frac{\sin\varphi_0(x,y)}{|x-y|} = \frac{1}{2}\cot\left(\frac{\theta-\theta_0}{2}\right) = \frac{1}{2}\frac{\mathrm{e}^{\mathrm{i}\theta}+\mathrm{e}^{\mathrm{i}\theta_0}}{-\mathrm{i}(\mathrm{e}^{\mathrm{i}\theta}-\mathrm{e}^{\mathrm{i}\theta_0})} = \frac{1}{2}\frac{\mathrm{e}^{\mathrm{i}\theta}-\mathrm{e}^{\mathrm{i}\theta_0}+2\mathrm{e}^{\mathrm{i}\theta_0}}{-\mathrm{i}(\mathrm{e}^{\mathrm{i}\theta}-\mathrm{e}^{\mathrm{i}\theta_0})} =$$
$$= \frac{1}{2}\left(\frac{1}{-\mathrm{i}} + \frac{2\mathrm{i}\mathrm{e}^{\mathrm{i}\theta_0}}{\mathrm{e}^{\mathrm{i}\theta}-\mathrm{e}^{\mathrm{i}\theta_0}}\right) = \frac{1}{2}\left(\frac{1}{-\mathrm{i}} + \frac{2\mathrm{i}t\cdot t_0}{t(t-t_0)}\right),$$

where $t = \mathrm{e}^{\mathrm{i}\theta}, t_0 = \mathrm{e}^{\mathrm{i}\theta_0}$.

Therefore, the integral equations (7), (11)

$$\frac{1}{\pi}\int_a^b \mu(\sigma)\frac{\sin\varphi_0(x(s),y(\sigma))}{|x(s)-y(\sigma)|}\mathrm{d}\sigma = -\frac{2f(s)}{1+\beta^2}, \quad \int_a^b \mu(\sigma)\mathrm{d}\sigma = 0,$$

can be written as

$$\frac{1}{\pi}\int_a^b \mu(\theta)\frac{1}{2}\left[\frac{1}{-\mathrm{i}}\mathrm{d}\theta + \frac{2t_0}{t(t-t_0)}\mathrm{d}t\right] = -\frac{2f(\theta_0)}{1+\beta^2}, \quad \int_a^b \mu(\theta)\mathrm{d}\theta = 0,$$

with $\dfrac{\mathrm{d}t}{\mathrm{i}t} = \mathrm{d}\theta;\ \sigma = \theta,\ s = \theta_0$. Consequently

$$\frac{1}{\pi}\int_{\exp(\mathrm{i}a)}^{\exp(\mathrm{i}b)} \mu(\theta)\frac{t_0}{t}\frac{\mathrm{d}t}{t-t_0} = -\frac{2f(\theta_0)}{1+\beta^2}, \quad \int_a^b \mu(\theta)\mathrm{d}\theta = 0.$$

Set $\dfrac{\mu(\theta)}{t} = \tilde{\mu}(\theta)$ and $\dfrac{2f(\theta_0)}{t_0}\dfrac{1}{1+\beta^2} = \tilde{f}(\theta_0)$; then the above equation becomes

$$\frac{1}{\pi}\int_{\exp(\mathrm{i}a)}^{\exp(\mathrm{i}b)} \tilde{\mu}(\theta)\frac{\mathrm{d}t}{t-t_0} = -\tilde{f}(\theta_0). \tag{60}$$

The solution of Eq. (60) is known (see [10, Sects. 85, 86]):

$$\tilde{\mu}(\theta_0) = \frac{1}{\pi}\frac{1}{q_1(t_0)}\int_{\exp(ia)}^{\exp(ib)} \frac{q_1(t)\tilde{f}(\theta)}{t-t_0}\mathrm{d}t + \frac{\gamma}{q_1(t_0)} \tag{61}$$

where $q_1(t) = \sqrt{\mathrm{e}^{\mathrm{i}\theta} - \mathrm{e}^{\mathrm{i}a}}\sqrt{\mathrm{e}^{\mathrm{i}\theta} - \mathrm{e}^{\mathrm{i}b}}$, γ is an arbitrary constant. The function $q_1(t)$ is the limit value of the function $q_1(z) = \sqrt{z - \mathrm{e}^{\mathrm{i}a}}\sqrt{z - \mathrm{e}^{\mathrm{i}b}}$ on the arc

$$\Gamma = \{z: \ |z| = 1, \ \arg(z) \in [a, b]\}$$

from the interior of the unit disk. In other words, $q_1(t) = q_1^+(t)$, where $q_1^+(t)$ is the limit value of $q_1(z)$ on Γ^+. The function $q_1(z)$ is an analytic function on the plane cut along Γ. The branch of the square root in $q_1(z)$ is taken in such a way that $q_1(z) \sim z$ as $z \to \infty$.

It can be shown that

$$q_1(t) = -2t^{\frac{1}{2}}\mathrm{e}^{\mathrm{i}\frac{a+b}{4}}\left|\sin\frac{\theta-a}{2}\right|^{\frac{1}{2}}\left|\sin\frac{\theta-b}{2}\right|^{\frac{1}{2}} = -t^{\frac{1}{2}}\mathrm{e}^{\mathrm{i}\frac{a+b}{4}}R_1(\theta),$$

where $R_1(\theta) = 2\left(\sin\frac{\theta-a}{2}\right)^{\frac{1}{2}}\left(\sin\frac{b-\theta}{2}\right)^{\frac{1}{2}}$. Therefore we obtain

$$\begin{aligned}\mu(\theta_0) &= \frac{1}{\pi}\frac{1}{q_1(t_0)}\int_{\exp(ia)}^{\exp(ib)}\frac{t_0}{t}\frac{q_1(t)f(\theta)}{t-t_0}\mathrm{d}t\left(\frac{2}{1+\beta^2}\right) + \frac{\gamma t_0}{q_1(t_0)} \\ &= \frac{1}{\pi}\frac{1}{R_1(\theta_0)}\int_{\exp(ia)}^{\exp(ib)}\frac{t_0^{1/2}}{t^{1/2}}\frac{R_1(\theta)f(\theta)}{t-t_0}\mathrm{d}t\left(\frac{2}{1+\beta^2}\right) + \frac{\gamma t_0}{q_1(t_0)}.\end{aligned}$$

Since $t - t_0 = \mathrm{e}^{\mathrm{i}\theta} - \mathrm{e}^{\mathrm{i}\theta_0} = 2\mathrm{i}t^{1/2}t_0^{1/2}\sin\frac{\theta-\theta_0}{2}$, $\mathrm{d}t = \mathrm{i}\mathrm{e}^{\mathrm{i}\theta}\mathrm{d}\theta = \mathrm{i}t\mathrm{d}\theta$, we get

$$\mu(\theta_0) = \frac{1}{\pi}\frac{1}{R_1(\theta_0)}\int_a^b \frac{R_1(\theta)f(\theta)}{2\sin\frac{\theta-\theta_0}{2}}\mathrm{d}\theta\left(\frac{2}{1+\beta^2}\right) + \frac{\gamma t_0}{q_1(t_0)}. \tag{62}$$

Obviously, $\mu(\theta_0)$ should be real, since it is a real solution of the real equations (7), (11). Since the integral in (62) is real, the function $\gamma t_0/q_1(t_0)$ should be real also; therefore $\gamma = 0$.

Finally, we get that the following function

$$\begin{aligned}\mu(\theta_0) &= \frac{1}{\pi}\left(\frac{1}{1+\beta^2}\right)\frac{1}{R_1(\theta_0)}\int_a^b\frac{R_1(\theta)f(\theta)}{\sin\frac{\theta-\theta_0}{2}}\mathrm{d}\theta = \\ &= \frac{1}{\pi}\frac{1}{q_1(t_0)}\int_{\exp(ia)}^{\exp(ib)}\frac{t_0}{t}\frac{q_1(t)f(\theta)}{t-t_0}\mathrm{d}t\left(\frac{2}{1+\beta^2}\right)\end{aligned} \tag{63}$$

is a solution to the system (7), (11) in our case. Indeed, it can be verified, using (60), (61), that the function (63) satisfies condition (7). Note that the system (7), (11) is equivalent to Eq. (14). Formula (63) coincides with (39).

Below we simplify formula (63) for certain functions $f(\theta)$. If $f \equiv 1$, we consider the singular integral

$$\frac{1}{\pi}\int_{\exp(ia)}^{\exp(ib)}\frac{q_1(t)}{t}\frac{\mathrm{d}t}{t-t_0} = \frac{\mathrm{i}}{\mathrm{i}\pi}\int_{\exp(ia)}^{\exp(ib)}\frac{q_1(t)}{t}\frac{\mathrm{d}t}{t-t_0} = (\Psi_1^+(t_0) + \Psi_1^-(t_0))\mathrm{i}, \quad t_0 \in \Gamma, \tag{64}$$

where

$$\Psi_1(z) = \frac{1}{2\pi\mathrm{i}}\int_{\exp(ia)}^{\exp(ib)}\frac{q_1(t)}{t}\frac{\mathrm{d}t}{t-z}, \quad z \notin \Gamma.$$

By the superscripts + and − we denote limit values of functions on Γ^+ and on Γ^-, respectively. Consider the function $q_1(z) = \sqrt{z - e^{ia}}\sqrt{z - e^{ib}}$, which is analytic outside Γ and such that $q_1(t) = q_1^+(t) = -q_1^-(t)$. Let $\Lambda = \Gamma^+ \cup \Gamma^-$ be a closed contour passing in a clockwise direction; then

$$\Psi_1(z) = \frac{1}{4\pi i}\int_\Lambda \frac{q_1(t)}{t}\frac{dt}{t-z}.$$

Let C_R be a circumference of a large radius R with the center in the origin; then

$$\int_\Lambda \frac{q_1(t)}{t}\frac{dt}{t-z} + \int_{C_R} \frac{q_1(t)}{t}\frac{dt}{t-z} = 2\pi i \sum \text{res} = 2\pi i\left[-\frac{q_1(0)}{z} + \frac{q_1(z)}{z}\right],$$

$$\lim_{R\to\infty}\int_{C_R} \frac{q_1(t)}{t}\frac{dt}{t-z} = \lim_{R\to\infty}\int_{-\pi}^{\pi} \frac{q_1(t)}{t-z} i d\theta = 2\pi i,$$

$$\Psi_1(z) = \frac{1}{4\pi i}\int_\Lambda \frac{q_1(t)}{t}\frac{dt}{t-z} = \frac{1}{4\pi i}\left[-2\pi i - 2\pi i\frac{-e^{i\frac{a+b}{2}}}{z} + 2\pi i\frac{q_1(z)}{z}\right],$$

because $q_1(0) = -e^{i\frac{a+b}{2}}$. Hence

$$(\Psi_1^+(t_0) + \Psi_1^-(t_0))|_\Gamma = \left[-4\pi i + 4\pi i\frac{e^{i\frac{a+b}{2}}}{t_0}\right]\frac{1}{4\pi i},$$

and it follows from (64) that

$$\begin{aligned}\frac{1}{\pi}\frac{1}{q_1(t_0)}\int_{\exp(ia)}^{\exp(ib)} \frac{t_0}{t}\frac{q_1(t)dt}{t-t_0} &= \frac{i}{q_1(t_0)}t_0\left(-1 + \frac{e^{i\frac{a+b}{2}}}{t_0}\right)\\ &= \frac{i t_0^{1/2}}{R_1(\theta_0)}\left(e^{-i\frac{a+b}{4}} - \frac{e^{i\frac{a+b}{4}}}{t_0}\right)\\ &= -\frac{2}{R_1(\theta_0)}\sin\left(\frac{\theta_0}{2} - \frac{a+b}{4}\right).\end{aligned}$$

Therefore, if $f \equiv \text{Const.}$, then Eq. (63) takes the form (41):

$$\mu(\theta_0) = -4\frac{\text{Const.}}{R_1(\theta_0)}\frac{1}{1+\beta^2}\sin\left(\frac{\theta_0}{2} - \frac{a+b}{4}\right).$$

Now, we evaluate the real integral (63) if $f(\theta) = A\cos\theta + B\sin\theta$. Since $t = \cos\theta + i\sin\theta$, consider the integral:

$$\frac{1}{2\pi}\frac{1}{R_1(\theta_0)}\int_a^b \frac{tR_1(\theta)}{\sin\frac{\theta-\theta_0}{2}}d\theta = \frac{1}{\pi}\frac{t_0}{q_1(t_0)}\int_{e^{ia}}^{e^{ib}} \frac{q_1(t)}{t-t_0}dt. \tag{65}$$

Consider the following jump problem: Find a piecewise-holomorphic function $\Psi_2(z)$ with the line of jumps Γ, so that $\Psi_2(\infty) = 0$ and $(\Psi_2^+(t) - \Psi_2^-(t))|_\Gamma = q_1(t)$.

The solution of this problem is given by the expression

$$\Psi_2(z) = \frac{1}{2\pi i}\int_{e^{ia}}^{e^{ib}} \frac{q_1(t)}{t-z}dt,$$

owing to Plemelj formulas [10, Sect. 16]. On the other hand, it can be verified directly that the function

$$\frac{1}{2}\left\{q_1(z) + \frac{e^{ia} + e^{ib}}{2} - z\right\}$$

is a solution of the jump problem as well. It is shown in [10, Sect. 31] that the solution of the jump problem is unique, consequently

$$\Psi_2(z) = \frac{1}{2\pi i}\int_{e^{ia}}^{e^{ib}} \frac{q_1(t)}{t-z}\mathrm{d}t = \frac{1}{2}\left\{q_1(z) + \frac{e^{ia}+e^{ib}}{2} - z\right\}.$$

Using Plemelj formulas [10, Sect. 16], we obtain for $t_0 \in \Gamma$:

$$\begin{aligned}\frac{1}{\pi}\frac{t_0}{q_1(t_0)}\int_{e^{ia}}^{e^{ib}} \frac{q_1(t)}{t-t_0}\mathrm{d}t &= \frac{it_0}{q_1(t_0)}(\Psi_2^+(t_0)+\Psi_2^-(t_0))|_\Gamma \\ &= \frac{it_0}{q_1(t_0)}\left[e^{i\frac{a+b}{2}}\cos\frac{a-b}{2} - t_0\right] \\ &= -i\frac{t_0^{1/2}}{R_1(\theta_0)}\left[e^{i\frac{a+b}{4}}\cos\frac{a-b}{2} - e^{-i\frac{a+b}{4}}t_0\right] \\ &= \frac{1}{R_1(\theta_0)}\left[ie^{i\left(\frac{3}{2}\theta_0-\frac{a+b}{4}\right)} - i\,e^{i\left(\frac{\theta_0}{2}+\frac{a+b}{4}\right)}\cos\frac{a-b}{2}\right],\end{aligned}$$

since $q_1(t) = -t^{1/2}e^{i\frac{a+b}{4}}R_1(\theta)$.

Taking the real and imaginary parts in (65), we get

$$\begin{aligned}\frac{1}{2\pi}\frac{1}{R_1(\theta_0)}\int_a^b \frac{R_1(\theta)\cos\theta}{\sin\frac{\theta-\theta_0}{2}}\mathrm{d}\theta &= \frac{1}{R_1(\theta_0)}\left\{\sin\left(\frac{\theta_0}{2}+\frac{a+b}{4}\right)\cos\frac{a-b}{2} - \sin\left(\frac{3}{2}\theta_0-\frac{a+b}{4}\right)\right\}, \\ \frac{1}{2\pi}\frac{1}{R_1(\theta_0)}\int_a^b \frac{R_1(\theta)\sin\theta}{\sin\frac{\theta-\theta_0}{2}}\mathrm{d}\theta &= \frac{1}{R_1(\theta_0)}\left\{\cos\left(\frac{3}{2}\theta_0-\frac{a+b}{4}\right) - \cos\left(\frac{\theta_0}{2}+\frac{a+b}{4}\right)\cos\frac{a-b}{2}\right\}.\end{aligned}$$

From these formulas we obtain (42).

A.4. Algorithm for the direct computation of the kernel of the angular potential

Algorithm 8.1 (Find the angular kernel V directly)

set $\xi_1 = a + h/2, \quad \mathrm{add} = 0$

$$\sin(\bar{V}(x,\xi_1)) = \frac{x_2 - y_2(\xi_1)}{|x - y(\xi_1)|}$$

if $\sin(\bar{V}(x,\xi_1)) > 0$

$$V(x,\xi_1) = \arccos\left(\frac{x_1 - y_1(\xi_1)}{|x - y(\xi_1)|}\right) + \mathrm{add}$$

elseif $\sin(\bar{V}(x,\xi_1)) < 0$

$$V(x,\xi_1) = -\arccos\left(\frac{x_1 - y_1(\xi_1)}{|x - y(\xi_1)|}\right) + \mathrm{add}$$

end

for $k = 2, \ldots, M$

$$\sin(\bar{V}(x,\xi_k)) = \frac{x_2 - y_2(\xi_k)}{|x - y(\xi_k)|}$$

if $\sin(\bar{V}(x,\xi_k)) > 0$

$$\bar{V}(x,\xi_k) = \arccos\left(\frac{x_1 - y_1(\xi_k)}{|x - y(\xi_k)|}\right) + \text{add}$$

if $(\bar{V}(x,\xi_k) - V(x,\xi_{k-1})) > \pi$

$$\text{add} = -2\pi + \text{add}$$

$$V(x,\xi_k) = \arccos\left(\frac{x_1 - y_1(\xi_k)}{|x - y(\xi_k)|}\right) + \text{add}$$

else

$$V(x,\xi_k) = \bar{V}(x,\xi_k)$$

end

elseif $\sin(\bar{V}(x,\xi_k)) < 0$

$$\bar{V}(x,\xi_k) = -\arccos\left(\frac{x_1 - y_1(\xi_k)}{|x - y(\xi_k)|}\right) + \text{add}$$

if $(\bar{V}(x,\xi_k) - V(x,\xi_{k-1})) < -\pi$

$$\text{add} = 2\pi + \text{add}$$

$$V(x,\xi_k) = -\arccos\left(\frac{x_1 - y_1(\xi_k)}{|x - y(\xi_k)|}\right) + \text{add}$$

else

$$V(x,\xi_k) = \bar{V}(x,\xi_k)$$

end

end

end

References

1. Lifanov IK (1996) Singular integral equations and discrete vortices. Zeist. VSP, International Sceience Publishers, The Netherlands
2. Lifanov IK, Poltavskii LN, Vainikko GM (2004) Hypersingular integral equations and their applications. CRC Press, Boca Raton
3. Hall EH (1879) On a new action of the magnet on electric currents. Am J Maths 2:287
4. Putley EH (1960) The Hall effect and related phenomena. Butterworth, London
5. Seeger K (1973) Semiconductor physics. Springer, NY
6. Sze SM (1981) Physics of semiconductor devices. Wiley, NY
7. Krutitskii PA, Krutitskaya NCh, Malysheva GYu (1999) A problem related to the Hall effect in a semiconductor with an electrode of an arbitrary shape. Math Prob Eng 5:83–95
8. Gabov SA (1977) An angular potential and its applications. Math USSR Sbornik 32:423–436
9. Krutitskii PA (1994) Dirichlet problem for the Helmholtz equation outside cuts in a plane. Comp Maths Math Phys 34:1073–1090
10. Muskhelishvili NI (1968) Singular Integral Equations. Nauka, Moscow and Noordhoff, Groningen (1972)
11. Krutitskii PA (1994) Neumann problem for the Helmholtz equation outside cuts in a plane. Comp Maths Math Phys 34:1421–1431
12. Belotserkovskii SM, Lifanov IK (1993) Method of discrete vortices. CRC Press, Boca Raton
13. Vainikko G (2001) Fast solvers of generalized airfoil equation of index 1. Operator theory: advances and applications 121:498–516
14. Saranen J, Vainikko G (2002) Periodic integral and pseudodifferential equations with numerical approximation. Springer, Berlin